166522

EFFECTS OF DRAWBEADS
IN SHEET METAL FORMING

M.Sc.Thesis by

Orhan ÇİÇEK, B.Sc.

Department :   Mechanical Engineering

Programme: Solid Mechanics

AUGUST 2005

İSTANBUL TECHNICAL UNIVERSITY ★ INSTITUTE OF SCIENCE AND TECHNOLOGY

EFFECTS OF DRAWBEADS
IN SHEET METAL FORMING

M.Sc.Thesis by
Orhan ÇİÇEK, B.Sc.

(503021513)

Date of submission : 1 September 2005

Date of defence examination: 8 August 2005

Supervisor (Chairman): Assoc. Prof. Dr. Erol ŞENOCAK

Members of the Examining Committee Prof.Dr. Mehmet Demirkol

Assoc. Prof. Dr. Halit S. TÜRKMEN

AUGUST 2005

ACKNOWLEDGEMENTS

TABLE OF CONTENTS

ABBREVIATIONS

BHF	: Binder Hold Down Force
CAD	: Computer Aided Design
DBRF	: Drawbead Restraining Force
FEM	: Finite Element Method
FEA	: Finite Element Analysis
FLC	: Forming Limit Curve
FLD	: Forming Limit Diagram
POL	: Punch Opening Line

LIST OF TABLES

LIST OF FIGURES

LIST OF SYMBOLS

E	: Young's modulus
F_N	: Effective blankholder force
H	: Bead height (bead penetraton)
K	: Material strenght
m	: Strain rate exponent
n	: Strain hardening exponent
P	: Effective blankholder force per unit length of the bead
r	: Normal anisotropy coefficient
R	: Bending radius
Rb	: Bead radius
Rg	: Shoulder radius of the groove
t	: Sheet thickness
ε	: Strain
σy	: Yield stress
θ	: Bending angle of the blank
w	: Sheet width
μ	: Coefficient of friction

SÜZDÜRME ÇUBUKLARININ METAL ŞEKİLLENDİRMEYE ETKİLERİ

ÖZET

Kırışma, yırtılma, aşırı incelme, yüzey bozunması ve geri yaylanma gibi kusurlar sac malzemede şekillendirme esnasında meydana gelen en bilindik kusurlardandır. Bu tür kusurlar genellikle sac malzemenin kalıp boşluğuna kontrolsüz ve istenmeyen bir oranda akışından kaynaklanmaktadır. Bir dizi yöntem sac malzemenin kalıp boşluğuna akışını kontrol etmede kullanılabilir: değişken potçemberi kuvveti uygulaması ve kalıp ile sac yüzeyleri arasındaki sürtünmenin azaltılması gibi. Fakat, bu yöntemler sadece sac malzemenin bütününün genel akışını düzenleyebilir. Sac malzemede meydana gelen kusurları azaltmak ve yok etmek için malzeme akışının belirli bölgelerde düzenlenmesi gerekmektedir. Bu, malzeme akış yollarını gerekli bölgelerde engelleyen bir tür yerel kontrol mekanizması olan süzdürme çubuğunun kullanılması fikrini doğurmuştur.

Bu çalışmada, süzdürme çubuklarının kullanımının sac şekillendirmeye etkileri incelenmiştir. Çalışmanın ikinci bölümünde süzdürme çubukları hakkında genel bilgiler sunulmuştur. Süzdürme çubuklarının çalışma prensipleri, metal şekillendirmede kullanılan tipleri ile kullanım yerleri ve bazı dezavantajları bu bölümde sunulmuştur. Üçüncü bölümde süzdürme çubuklarının oluşturduğu kuvvet değerlerinin belirlenmesinde kullanılan bir dizi analitik süzdürme çubuğu modeli ele alınmış ve bu modellerde yapılan kabuller ile bunların doğruluk dereceleri gösterilmiştir. Dördüncü bölümde ise bu analitik modellerden en yaygın kullanılanı üzerinde durularak süzdürme çubuğu kuvvetlerine proses değişkenlerinin etkisi incelenmiştir. Beşinci bölüm süzdürme çubuklarının sayısal modellenmesini içermektedir. Süzdürme çubuğu kuvvetlerinin belirlenmesinde 3B düzlem gerilme ve 2B düzlem şekil değiştirme sonlu elemanlar modelleri oluşturulmuştur. Çözüm süresini ve optimizasyon çevrimini azaltmak amacıyla sonlu elemanlar uygulamalarında sıkça kullanılan ve gerçek süzdürme çubuklarının yerine kullanılan eşdeğer süzdürme çubuğu modeli de bu bölümde ele alınmıştır. Analitik ve sayısal sonuçlar litaratürdeki deneysel verilerle karşılaştırılarak sunulmuştur. Altıncı bölümde ise süzdürme çubuğu kullanımının metal şekillendirmeye etkisi ile eşdeğer süzdürme çubuğu modelinin doğruluk derecesi iki ayrı sonlu elemanlar uygulamasına yer verilerek gösterilmiştir. Uygulamalar gerçek süzdürme çubuğunun olduğu ve olmadığı durum ile eşdeğer süzdürme çubuğunun olduğu durum ele alınarak çözülmüştür.

EFFECTS OF DRAWBEADS IN SHEET METAL FORMING

SUMMARY

The defects such as wrinkles, fractures, excessive thinning surface distortion and springback are common failures that usually occur on the sheets during a sheet metal forming process. Such failures are caused by the use of an unwanted flow rate of the sheet material. A number of techniques can generally be used to control the flow rate of the metal sheet: regulating the blank holder force and reducing the friction between the die and metal sheet surfaces. However, these techniques can only be used to regulate the overall flow rate of the whole metal sheet. In order to minimize tears and wrinkles, it is necessary to regulate the flow rate at certain parts of the sheet. This leads to the idea of using a drawbead to obstruct the flow path in order to achieve control over the flow rate at the necessary locations.

In this thesis, the effect of using drawbeads in a sheet metal forming process is investigated. Chapter 2 contains the description of the basics about drawbeads. The working mechanism of drawbeads, the types and location of drawbeads used in sheet metal forming and disadvantage of using drawbeads are presented in this chapter. In Chapter 3 a number of analytical drawbead models are reviewed. The accuracy and assumptions made in these models are demonstrated. In Chapter 4, by concerning one of these models, the effects of parameters in drawbead forces are investigated. Chapter 5 presents the numerical modeling of drawbeads. 3D plane stress and 2D plane strain FE models are constructed in order to determine the drawbead forces. Equivalent drawbead modeling which is used instead of the real drawbead geometries to reduce huge computational time and optimization cycles in sheet metal forming simulations is also taken into account in this chapter. Analytical and numerical results are compared with the literature experimentally determined data. Chapter 6 deals with two FEA applications. The effect of drawbeads in industrial application and the accuracy of equivalent drawbead modelling are shown in this chapter. In the the simulations, the results in which the real drawbead geometry and its equivalent representation are taken into account are shown.

1. INTRODUCTION

One of the most common methods of shaping sheet metal into desired shapes is sheet metal forming which concerns the case where the thickness of the piece of material is small compared to the other dimensions. The sheet metal forming process is applied with the intention of manufacturing a product with a desired shape and no failures. The final product shape after sheet metal forming is defined by the tools, the blank and the process parameters. An incorrect design of the tools and blank shape or an incorrect choice of material and process parameters can yield a product with a deviating shape or with failures. A deviating shape is caused by elastic springback after forming and retracting the tools. The most frequent types of failure are wrinkling, necking (and subsequently tearing), scratching and orange peel.

In sheet metal forming process, a piece of material is plastically deformed between tools to obtain the desired product. Many different modes of deformation are employed to impart the specified shape to the sheet metal during stamping, such as stretching, bending, deep drawing, etc. In these forming modes, some defects such as wrinkling, splitting, excessive thinning may occur on the stamped sheet material. Wrinkling may occur in areas with high compressive strains, necking may occur in areas with high tensile strains, scratching is caused by defects of the tool surface and orange peel may occur after excessive deformations, depending on the grain size of the material.

Typically, a forming operation involves combinations of these different forming modes. Ability of the material to undergo these different forming modes without defects is broadly termed as the "formability" of the material. Formability is a system characteristic depending on material properties, die geometry, lubrication conditions, press speed, and restraint conditions caused by binder pressure and/or drawbeads.

A commonly used sheet metal forming process is the deep drawing process. Principle of deep drawing is schematically represented in Figure 1.1.
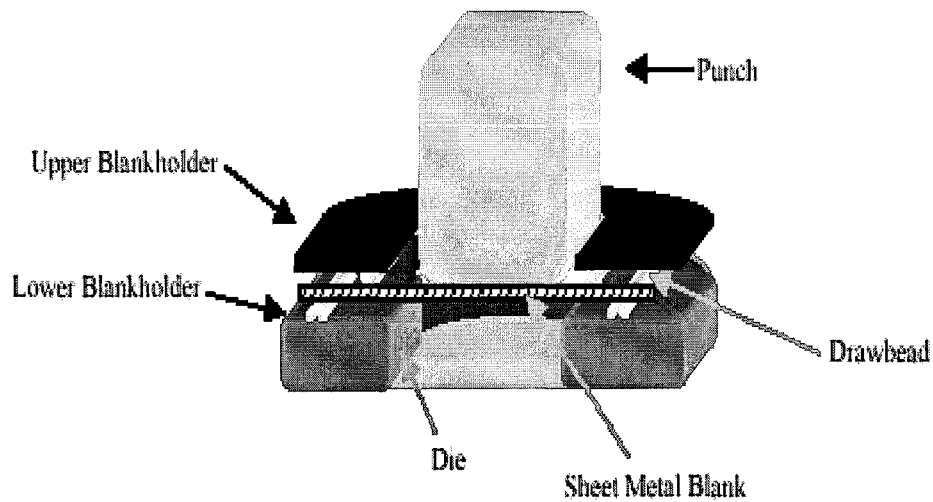
Figure 1.1: Schematic of the Deep Drawing Process

In the forming process, an initially flat or pre-shaped sheet material called blank is placed between a blank holder and a die. The blank holder is loaded with a force to prevent wrinkling and to control the amount of material that flows into the die. After that the punch is moved downwards, pushing into the blank, which then partly stretches, and partly pulls material from under the blank holder into the die. During the forming stage the material is drawn out of the blankholder-die region, whereas the material is subjected to compressive and tensile stresses during forming. The result of the process is a product which contains both the shape of the punch and that of the die. During the forming process, the flow of the material into the die is essential for the formability of the product and its properties.

Obtaining a wrinkle-free part and the desired percentage of stretch in a stamped part sometimes can be very costly and time-consuming. Wrinkles, fractures, loose metal, buckles, excessive thinning, fracture, surface distortion and springback are everyday problems in the sheet metal forming industry.

Addressing these difficulties requires a good understanding of metal flow and how it is affected by drawbeads which are most effecient local control mechanism. This thesis focuses on the principles of specifying, designing, and effects of drawbeads in sheet metal forming process.

2. DRAWBEADS

The quality of a stamped commercial part is largely influenced by the material flow within the tools during the sheet metal forming operation. Therefore it is important to control the material flow rate to avoid defects such as wrinkling, tearing, surface distortion and springback. Furthermore, in car body manufacturing it is important that outer panels should be subjected to sufficient straining because of the flex resistance (or dent resistance) [1]. Often, it is desirable to increase material flow by using lubricants to reduce stress. In other situations, it is common practice to reduce flow by introducing additional restraining force.

Generally, the material flow is controlled by the blankholder: a restraining force is created by friction between the tools and the blank. As a result, the tensile stresses are increased, material flow is controlled, and the formation of wrinkles is avoided. (see Figure 2.1)
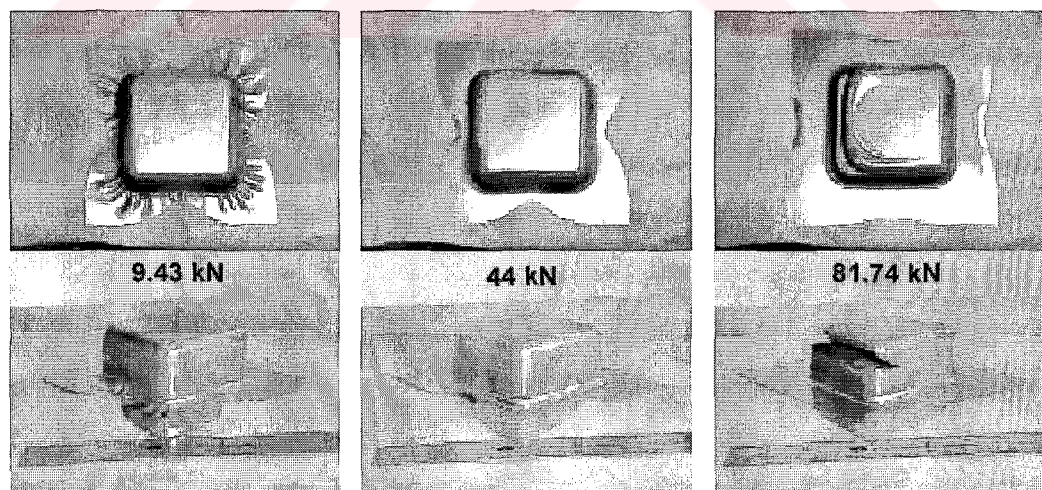
Figure 2.1: Effect of Blankholder Force on Formability of the Material.

However, during the forming stage, the blankholder does not make contact with the entire blank which means that it cannot fully control the material flow [2]. Moreover, when a higher restraining force is needed, higher blankholder force must be applied.

To reduce the flow of material between the binder faces or increase restraining force, it is not good practice to simply keep increasing the blankholder force. This results in higher stress values being imposed on the die and press which may cause excessive wear in the tools and galling in the blank and will reduce the cost effectiveness of the operation.

Furthermore, in same cases the minimum blankholder force required to provide the necessary restraining force for a successful drawing operation may exceed the tonnage capacity of the press. Therefore, a local control mechanism is desired which restrains the material flow sufficiently at relatively low blankholder force. These demands can be fulfilled by drawbeads, which are rib-like projections mounted on either the binder or the draw ring surface that restrict and control metal flow into the die cavity and over the punch of a draw die (see Figure 2.2). Drawbeads are an important characteristic of blankholder control and are used to supplement friction and obtain more uniform deformation.
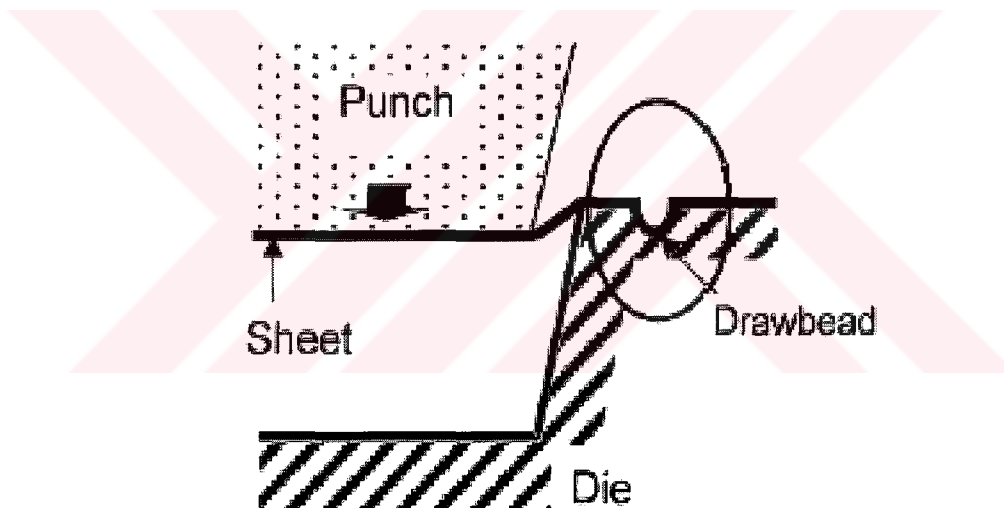
Figure 2.2: Schematic of a Stamping Process Including Drawbeads

2.1 Drawbead Working Mechanisms

The drawbead applies two types of forces are schematically represented in Figure 2.3: a drawbead restraining force (DBRF) and binder hold down force (BHF) which are related to the drawbead geometry (shape and dimension), sheet material (thickness and mechanical properties and process parameters.

4
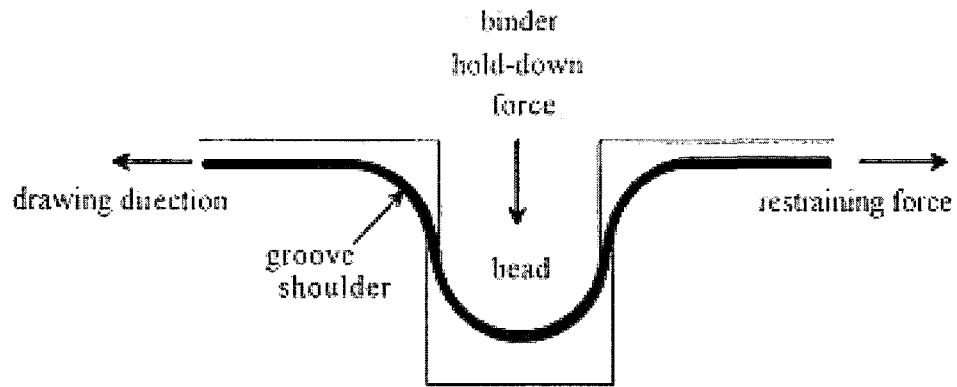
Figure 2.3: Drawbead Forces: Drawbead Restraining Force (DBF)
and Binder Hold Down Force (BHF)

The drawbead restraining force appears onto the blank by cyclically bending and unbending the sheet as it traverses the drawbead, causing strain hardening and a change in the strain distribution with consequently thinning of the blank. The direction of the DBRF is opposite to the material flow with the restriction that it acts perpendicular to the drawbead.

The binder hold down force (BHF) represents the force applied by the blank on the blank holder when the blank slides in the drawbead. The direction of the BHF, which appears when the material is pulled through the drawbead, is opposite to the blankholder force direction. This BHF causes a rise of the entire blankholder from which it can be concluded that the BHF is not a local phenomenon but will affect the total deep drawing process. The binder hold down force is therefore subtracted from the total blankholder force during the deep drawing simulation [3].

Figure 2.4 shows a traditional half-round bead machined or inserted into the top half of the die. The drawbead forces depend on the bead/groove design (see Figure 2.4), which consists of

1) radii of the groove shoulders

2) radii of the bead

3) cavity and clearance tolerances

4) material and process parameters
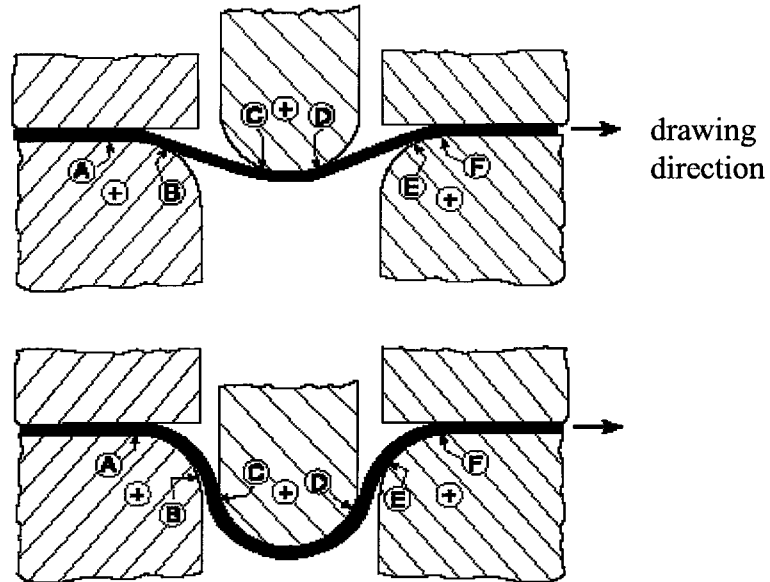
Fig 2.4: Schematics of a Round Drawbead at 30 % (top) and 100 % (bottom)
Penetration.

The top and bottom sketches in Figure 2.4 show 30% and 100% bead penetration, respectively. However, both deformation sequences are identical. Beginning at the bottom of the schematic, the sheet metal at point A bends to conform to the entry radius of the groove. Two things happen. First, a force is required to bend the sheet. The force is proportional to the R/t (bend radius to material thickness) ratio. Thus, a greater force is required to bend the sheet to a smaller radius. Second, the plastic deformation during bending causes the material to work harden. At point B the sheet becomes straight again. Another force is required to straighten the sheet, but the force now is greater than at point A because of the prior work hardening [4].

In addition, the unbending at B imparts yet a second increment of work hardening. The sequence repeats during the bending (C) and unbending (D) around the bead and yet a third time (E and F) around the exit radius of the groove. If the groove and bead have different radii, then the force to bend/unbend and the increment of work hardening will differ for each radius. The restraining force created by the bead is obtained by adding all the deformation forces and the work hardening increments (A through F). The 100 % penetration of the bead (Figure 2.4 bottom) looks much more severe than the 30 % penetration because of the increased angle of wrap. The angle of wrap for the entry radius can be seen as the arc distance between A and B, which is greatly increased for the 100 % penetration. However, the increased wrap angle

does not change the amount of force to bend and unbend the sheet or increment of work hardening. The material simply slides along the bead without additional deformation. A second, but small, contributor to the restraining force is the frictional force as the metal slides over the three radii. As the percent-penetration increases, the coefficient of friction does not change. However, as the angle of wrap increases, the force normal to the sheet increases, increasing the frictional force. Substituting a square bead with round corners (rectangular cross section) in place of the round bead will increase the restraining force. Now four bend-unbend sequences are required instead of three. In other words, the total number of bending and unbending deformation is eight for a square (or rectangular) and six for a round (semi-circular) drawbead. Assuming the square bead goes into the same bead cavity as the round bead, the corner radii of the square-bead are much smaller, thereby decreasing the R/t ratio and increasing the force to bend-unbend the sheet at the bead contours. The metal also undergoes greater work hardening and a greater frictional force.

2.2 Drawbead Shapes

A drawbead is composed of two components: a bead on one binder surface and a matching groove on the opposite binder surface, see Fig.2.5. The drawbead efficiency is mainly determined by the drawbead geometry. The radii of the drawbead and clearances between the bead and the shoulder can be varied, but also the shape of the cross-section.

Blankholder (Binder surface)

Die (Binder surface)
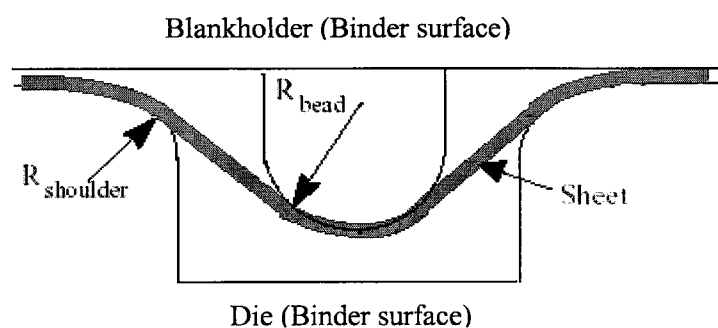
Figure 2.5: A Semi-circular Drawbead (Half-round Drawbead)

The shape of the cross-section can be round (semicircular), rectangular or non-symmetric (step or edge bead), see Figure 2.6. With semicircular drawbeads the radius is symmetrical whereas with rectangular drawbead the inlet and outlet radii may be different.

7
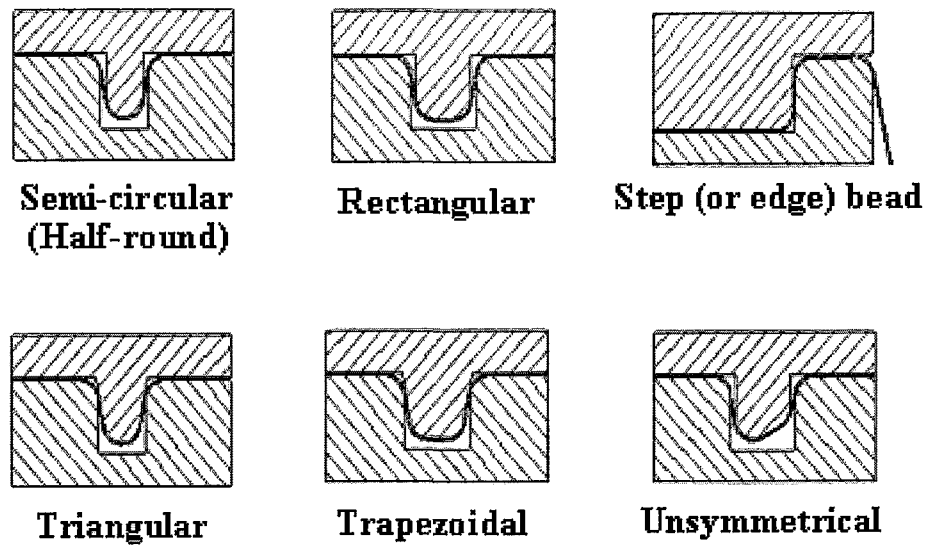
Figure 2.6: Cross-sections of Drawbead Shapes

Using rectangular drawbead or adding a flat-bottom section to the drawbead profile as shown in Figure 2.7 is one of the ways to increase drawbead restraining force. Figure 2.7 shows a drawbead geometry adding a flat-bottom section to its profile which introduces an additional bend/unbend sequence as in the rectangular drawbead geometry where the material is subjected to four bending and unbending sequences, whereas in the semi-circular drawbead geometry the material is subjected to three bending and unbending sequences.
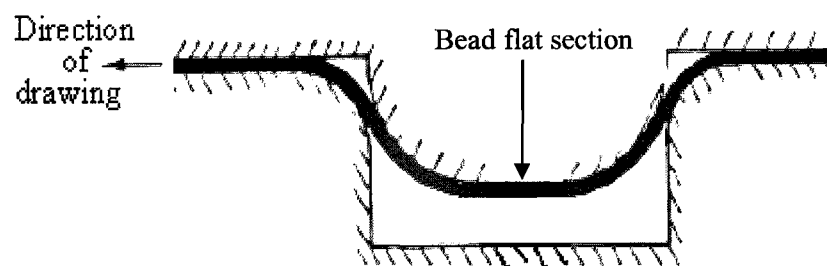
Figure 2.7: Drawing of a Flat-bottom Drawbead

Therefore, the drawbead with a rectangular cross-section will lead to a higher restraining force provided that the bending radii are the same. However, in practice, since the radii of a rectangular drawbead are smaller that the radius of a semi-circular drawbead, higher strains are produced during bending over the bead radii. This causes higher surface damage on the sheet and tool, and for a critical bead radius fracture may occur on the sheet.

Another characteristic of the rectangular drawbead is that it is relatively insensitive to lubrication. The blank does not follow the rectangular drawbead geometry at the top of the bead during forming, but creates a small cavity between the tool and the blank. This cavity is situated between the two radii of the bead and becomes a depot for the lubricant which is easily squeezed out of the contact areas due to this cavity [5].

Using the subsequent drawbeads (double row) is an another method to offer further drawbead restraining force for local additional control (see figure 2.8). There are two advantages; one is that it requires less blankholder force than a single drawbead that will give equivalent control. Second is that it is less likely to cause component splitting, but this method requires increased sheet blank size.

first drawbead   second drawbead
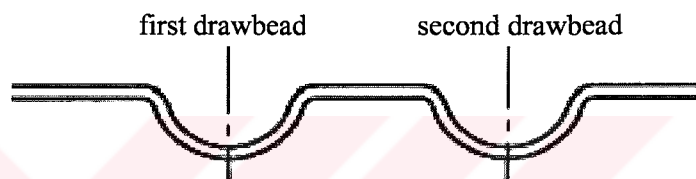
Figure 2.8: Double Row Drawbead Application

It is also possible to increase drawbead forces by inserting a hard urethane strip in the groove. This method is attractive in stamping processes including drawbeads with relatively shallow penetration. The urethane strip forces the sheet to conform more closely to the bead radius, increasing the bending deformation [6]. In practice, complex bead shapes add machining cost and force the sheet metal to conform to a more elaborate shape and can lead to tearing before metal flow through the bead begins.

When a step or edge bead is used, the total number of bending and unbending deformations is only four but the bending angle is 90 full penetration and the clearance is equal to the sheet thickness. Therefore, the effective bending radius the curvature of the bent sheet is equal to the tool radius, and a maximum restraining force is produced for a given tool radius. Another advantage of the step bead is that it can be located at the edge of the die corner so that material loss could be reduced. However, step beads often cast on the binder. Therefore, the wear and the necessary grinding to adjust metal flow may destroy the die wrap and the performance of the

total drawing action. Other problems may be (a) the possibility of fatigue fractures on the die when the drawbead is very close to the die corner, and (b) the cost of machining and altering of the step beads if the restraining force has to be modified [2]. Step beads around the blankholder edge should be used wherever possible due to metal economy.

The cross-section of drawbead may vary with side angle as shown in Figure 2.10. Drawbeads with triangular or trapezoidal geometry are also commonly used for this purpose (see also Figure 2.6). The blank holding action of a triangular bead with a corner radius of R_{g1} is the same as a semi circular bead with a radius of R_{g2}, if $R_{g1}=$ R_{g2}. Therefore, they produce equal restraining forces. The same is true for rectangular and trapezoidal beads; the blank holding action of a trapezoidal bead with corner radii of R_{g3}, is the same as a rectangular bead with corner radii of R_{g4}, if $R_{g3}= R_{g4}$ [1].
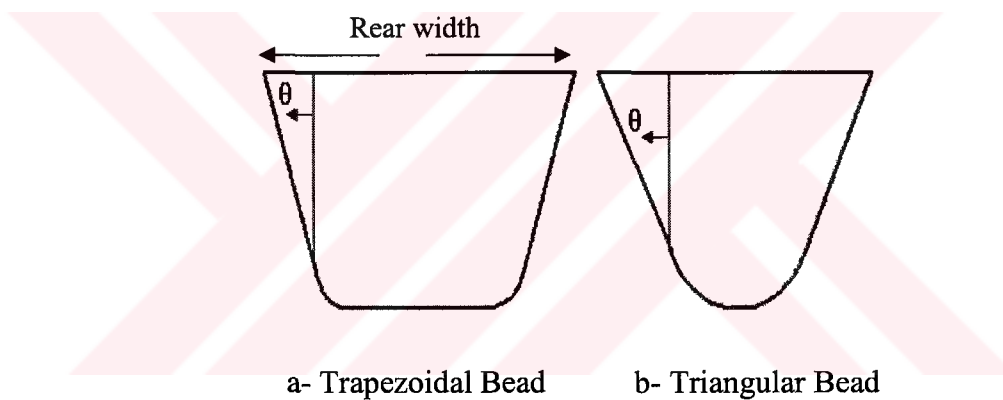
Figure 2.9: Drawbead Shapes: Trapezoidal and Triangular Bead

Triangular and trapezoidal beads are used for constructional and design purposes because their rear width can be adjusted by changing the side angle, θ

Another type of drawbead is lock bead or lockstep: in stretch forming, the sheet metal is firmly clamped and no material flow is allowed. Therefore a lock bead is required to provide the necessary restraining force to lock the sheet where stretch is required. Generally lock bead and lockstep have rectangular cross sections. Figure 2.10 shows the typical lock bead and lockstep and their sizes.
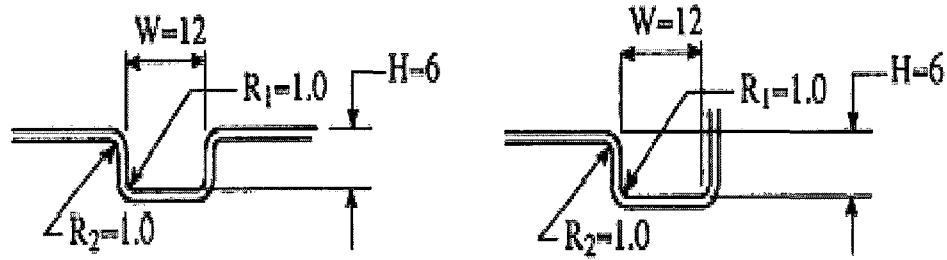
Figure 2.10: Drawbead Shapes: Lock bead and Lockstep and Their Sizes

Lockbead should be in straight lines wherever possible. When this is not possible any curvature should be kept to an absolute minimum. Locksteps around the blankholder edge should be used wherever possible due to metal economy. The bedding in the area between the lockbead and the die cavity radius is used to relieve the pressure at the bead radius thus helping to prevent splitting.

Optimization of drawbead performance can be achieved by adjusting the deformation in the sheet passing through the beads. Researchers at Michigan Tech are developing so-called dynamic drawbeads that can be moved via hydraulic actuators instead of conventional static drawbeads that are fixed in place. This new approach will allow the user to vary the restraining forces created by the drawbeads during deformation. Some results from their tests show that it is possible to form aluminum with deeper draws than with conventional fixed drawbeads. The next step in this development is to create what they term an "intelligent stamping die", capable of sensing problems in the forming process and adjusting the drawbeads accordingly [6].

2.3 Location of Drawbeads

In the tooling design of outer panels, the geometry of drawbead and its location will affect the distribution of restraining force along mouth of dies and relative flowing velocity of the blank, and consequently, will affect the distribution of strain and thickness in a formed part. Therefore, reasonable design and location of drawbead is the key point of outer panels' forming quality. With a proper positioning and design of drawbead, not only better formability and high dent resistance are obtain, but also fine cutting contour line and high assembly quality can be obtained.

Drawbeads are placed in the binder surface of a die to control metal flow. In the Figure 2.11 Figure, the left view shows the part formed with the problems, while the right view shows the part formed with corrective drawbeads. Figure 2.11 illustrates how unrestrained material can move too fast and may run inside the trim line (A) or generate buckles that fold over and jam between the punch and die ring (B). Here, drawbeads are more accurately described as speed bumps. Drawbeads also can create a back tension to help pull out loose metal or provide additional stretch and work hardening to the material inside the die opening (C). In this case, the drawbeads should be called stretch beads [7].
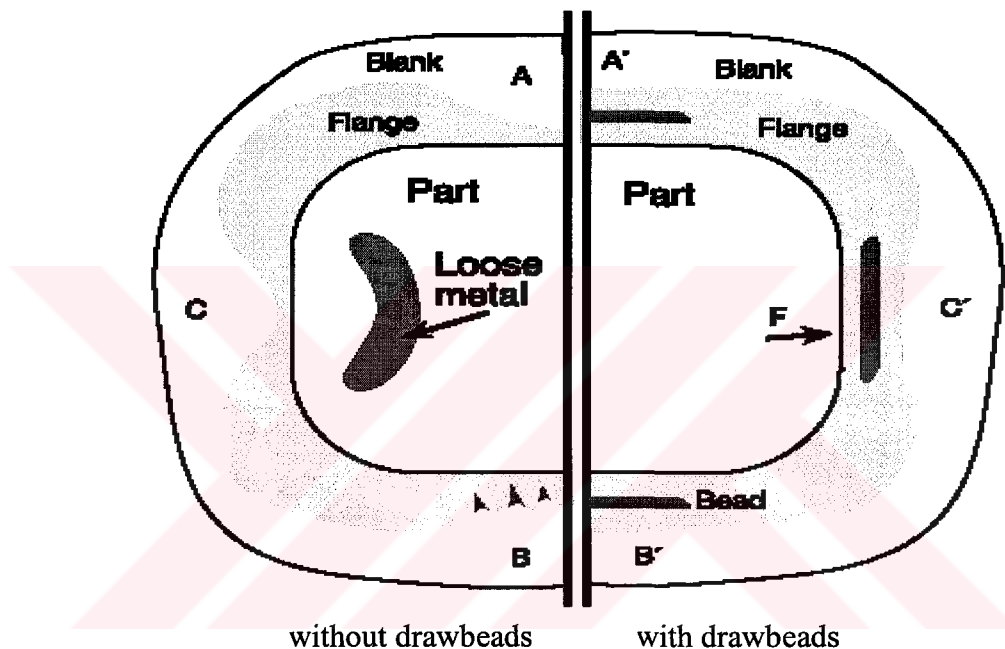
Figure 2.11: Plan View of a Rectangular Box Formed From a Developed Blank

Potential defects corrected by drawbeads are: uncontrolled flange material flow (A), large flange buckles (B) and loose material central to the part (C).

Determining the best location for a drawbead is a judgment call based primarily on part geometry. Deeper areas of a die require more material flow; shallow areas of the die consume less material. The best location for a drawbead can be predicted by the finite element (FE) calculation. Material consumption between the two surfaces can also be estimated experimentally using length-of-line analysis.

To keep excess material from flowing into the shallow areas of a part, drawbeads must be designed in the feeding areas of the binder surface. Experimenting with

sandpaper or grit cloth between the binder and draw ring surface can help determine the best location for a drawbead. Because of their abrasive natures, the materials act as grippers to help hold material and prevent it from going into the die cavity, thus mimicking drawbeads [7].

Another experimental process to help determine the best location for a drawbead involves increasing the blank size in the proposed area. The additional material between the binder and the draw ring increases the drawbead restraining force and indicates where a drawbead can be substituted.

The location of the drawbeads is crucial to their effectiveness. To obtain the maximum effect from the drawbead it should be close to the area requiring restraining and perpendicular to the flow of material.

Drawbeads generally achieve maximum effect of control when placed perpendicular to the flow of material (see Figure 2.12). This can be examined by the marks made on the drawn shell by the beads.

Drawbead not perpendicular to flow   Drawbead perpendicular to flow
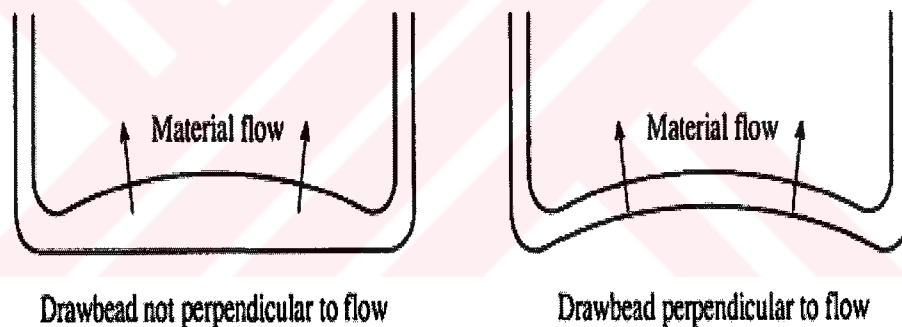
Figure 2.12: Drawbead Placement with Respect to Material Flow

To reduce the flow of material between the binder faces, it is not good practice to simply keep increasing the pressure. This results in higher stress values being imposed on the die and press and will reduce the cost effectiveness of the operation. Instead, the drawbead should be adjusted in accordance with the analysis of panel movement.

Where there is a possibility that an increase in die radius could reduce the effectiveness of the land (bedding area) between the bead and the die cavity this should be taken into account when positioning the bead. This is particularly important if the draw wall is an open angle and especially with curved punch/box

lines. Care should be taken to ensure that material pulled through the drawbead does not form part of the finished component.

The bedding area between the drawbead and the die cavity radius is used to maximise drawbead forces whilst minimising blankholder force. The bedding area outside the bead is used to prevent corrugations during material movement.

If the draw-wall is an open angle, the drawbead should be as close as practical to the POL as the component material will be unsupported during the forming operation and will therefore require tighter control. This is especially true if the POL has curvature [8].

If the drawbead is too far from the trim line and/or punch opening line (POL), as in the case of dimension "X" as shown in Figure 2.13, then the drawbead is unable to supply sufficient restraining force to control the material during forming.
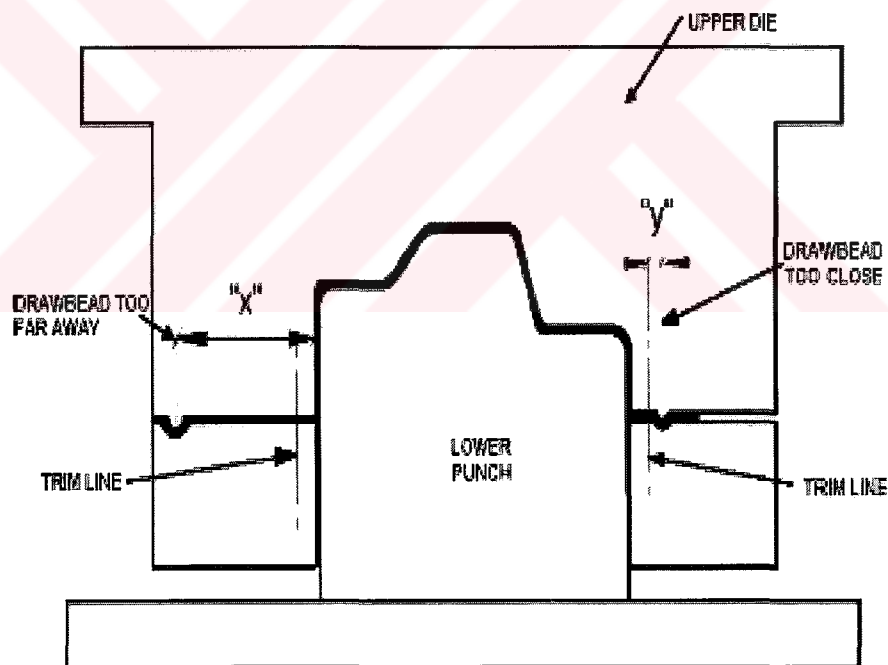
Figure 2.13: Position of Drawbeads

Conversely, as in the case of dimension "Y", if the bead is too close to the trim line or to the die cavity radius, material is saved, however material pulled over the bead can end up inside the trim line, and will be visible on the finished product. If the distance (the bedding area) is too short fatigue cracks may occur in production [9].

Drawbeads usually are not beneficial in the the corners of the binder. Many times, drawbeads are placed in the corners of the binder, where material already has a difficult time compressing and moving toward the die-opening line. Here, a drawbead restricts such movement and increases the punch force needed to maintain motion. The excessive punch load can result in wall or radius tearing.

In practice, a distance of 1.5 to 2 times the width of a bead to the die corner is recommended [10]. In order to avoid penetration into the zone of stress concentration, and hence, possible cracking, drawbeads are not located beyond a distance of 10° from the centre of the corner radius shown in Figure 2.14.
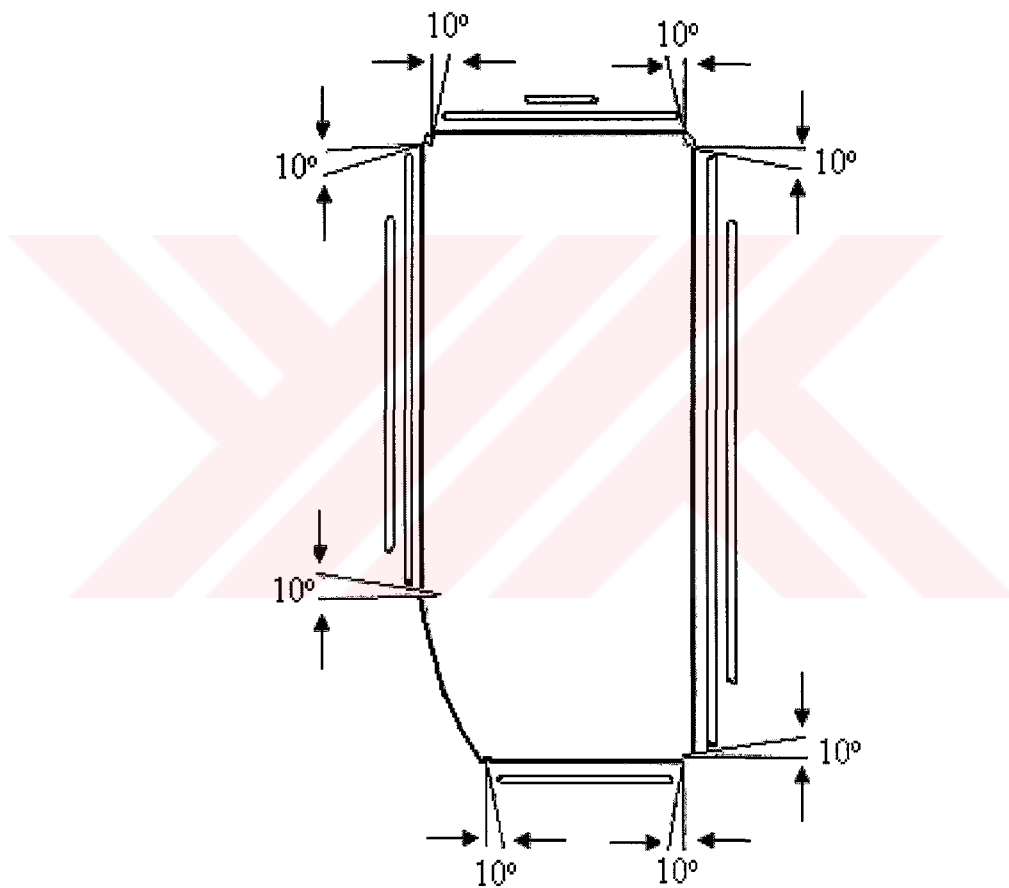
Figure 2.14: Position of Drawbeads for Rectangular Panels

In forming complex or rectangular parts, it is desired to increase the restraining force locally in the "easy flow" regions. On the other hand, the restraining force should be locally reduced where the sheet matal can not easily flow into the die cavity (i.e. corner of a rectangular panels) as shown Figure 2.15 and 2.16.
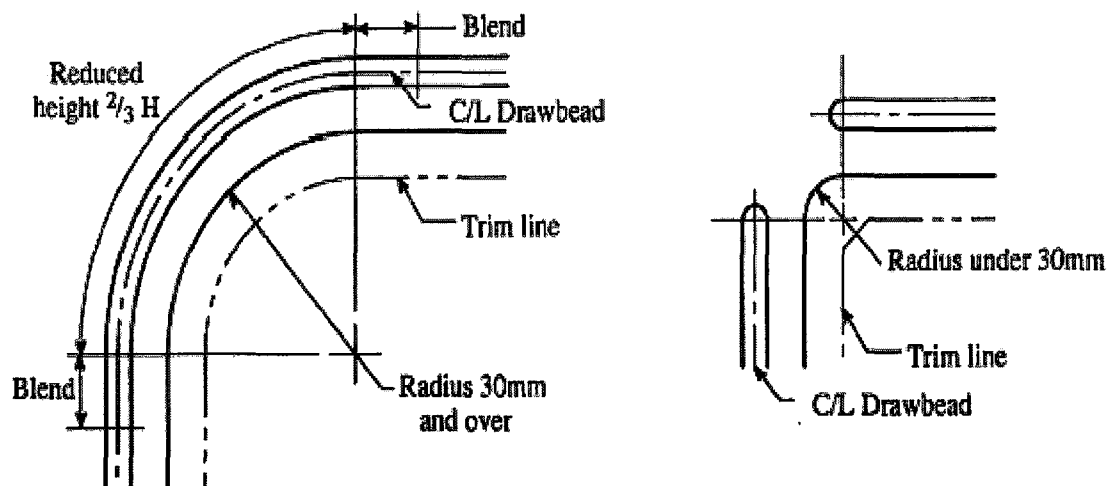
Figure 2.15: Position of Drawbeads: Trim Line on Punch

In the case of wrinkling and tearing on the corner of rectangular complex parts, there are two commonly drawbead setting on binder surfaces; using a drawbead design with reduced bead penetration, value of 2/3 bead height, with blended regions on the corner of punch shown in Figure 2.15. Another usage of drawbead design is shown in Figure 2.16.
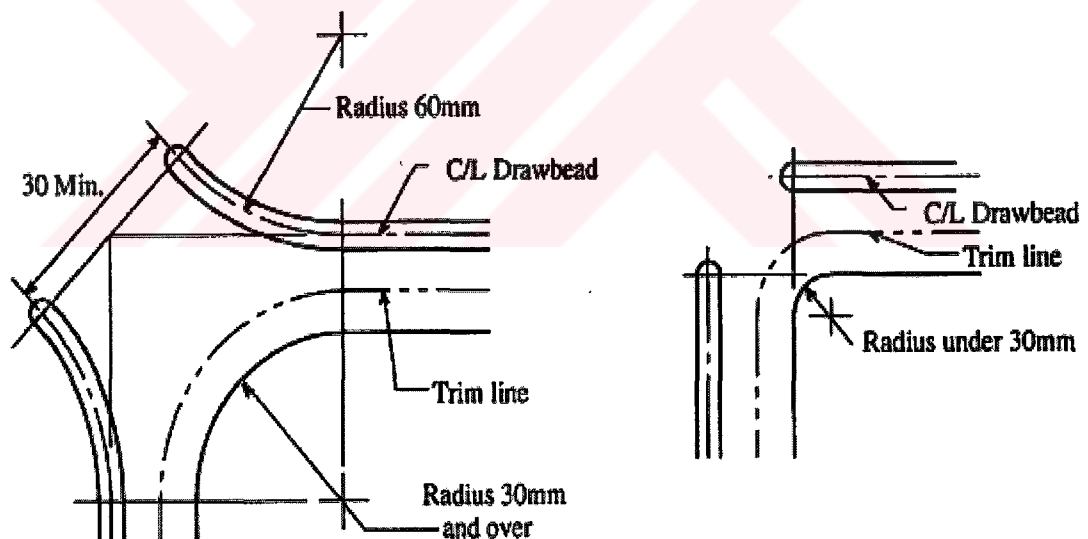
Figure 2.16: Position of Drawbeads: Trim Line on Blankholder

Drawbead must blend gradually into the surface on which they are located (see Figure 2.15-16). This blended transition gradually changes the restrictive force, reducing the possible shearing or tearing action of the "rind" or addendum areas of the drawn shell [11].

2.4 Mountining and Maintenance of Drawbeads

Because drawbeads usually are subjected to a great deal of abrasive and adhesive wear, they must be made from very wear-resistant tool steel. Steel with a carbon content of 1% is preferred [10] as drawbead material so that each piece can suitably be hardened and polished on the contact surfaces. Hardness of drawbead can be HRC >50. Working surface of drawbead causing material sharply deformation should be surface-treated to improve its life time and forming quality. A check is essential to make sure that there is no distortion after heat treatment. The bowing of a section can cause awkward problems and the only way to overcome this problem is to grind all the surfaces prior to a final polishing process. The surface roughness, R_a, should not exceed 0.25 μm (10 μin) [12].

Drawbeads can be machined, welded, or inserted on top of or into the draw ring or binder surface of a draw die. Male part of the drawbead (bead) can be mounted both on the upper die or the lower die [13]. Two main advantages of mounting the drawbeads on the upper die are that:

a) the working conditions are better on the lower die on which most of the remachining is done. Therefore, the beads are placed on the upper die where a minimum amount of remachining is done. The lower die area below the drawbead should not be fitted as this is detrimental to controlling drawbead force.

b) the grooves are on the lower die; hence, it is easier to rework them. However in this case, the beads must be locked to the upper die by screws or rivets. Thus the depth of the beads (penetration) can not be changed simply by shimming. Another disadvantage is that the groove cavities in the lower die can be easily filled with dirt.

The alternative is to locate the beads on the lower die where the beads do not need to be locked by screws or rivets. The depth of the bead can not be modified by shimming. Also, the beads can be remove in a relatively simple manner when die maintenance work is needed [1]. However, this procedure also has some disadvantages such as;

i) cratches (originating from the beads) may drawn down to the die edge, radius and contribute to bad appearances on the outer surface of the formed part,

ii) working conditions are more difficult when work needs to be done on the groove,

iii) beads may contribute to difficulties in blank feeding because the blank rests on the beads.

Drawbeads can either be cast or inserted into the binder rings (see Figure 2.17). The following factor must be considered in selecting the bead design [14]:
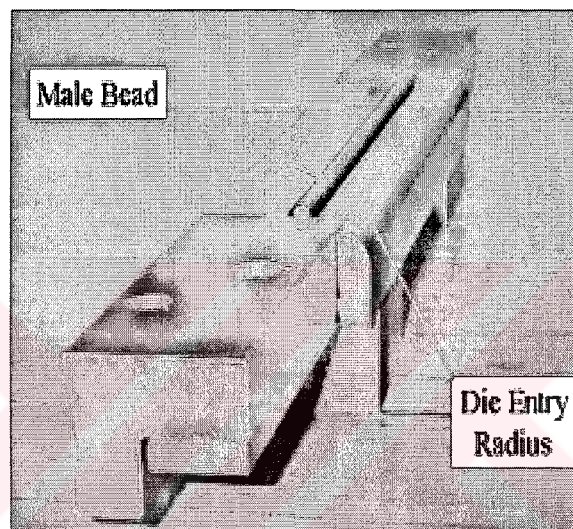
Figure 2.17: Interchangeable Drawbead Insert

i) Inserted male drawbeads at the die edge (inserted edge bead) can not be adequately supported.

ii) Inserted drawbeads permit the use of differential material to prevent galling.

iii) Inserted drawbeads are difficult to install when changing the bead pattern to modify the restraining force.

iv) The bead height (penetration) of an inserted bead can easily be changed.

v) Cast beads are successfully welded while inserted beads are subjected to warpage or loosening.

vi) If an increase in the restraining force is required from a cast drawbead, one has to either increase the blankholder force, which may not be feasible because of press tonnage limitations, or insert additional beads, which is costly and time consuming.

For ease of machining drawbeads should always be cut perpendicular to base of tool and not angled blankholder surface (see Figure 2.18).

a) Semi-circular drawbead   b) rectangular drawbead
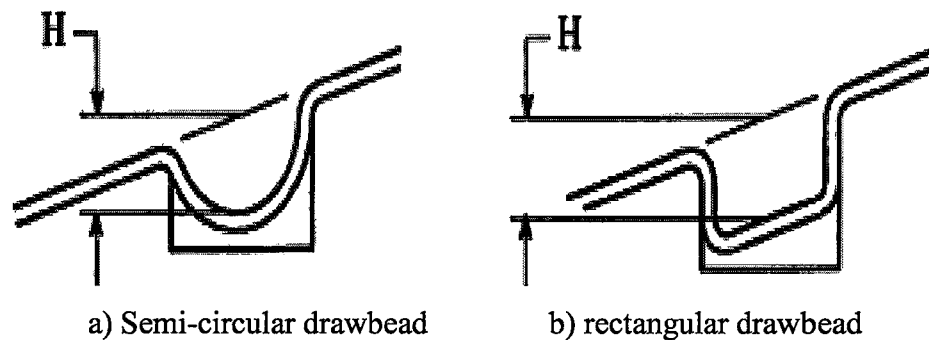
Figure 2.18: Mountining of Drawbeads

2.5 Disadvantages of Drawbeads

The use of drawbeads in sheet metal forming processes can have negative consequences. Very strong restraining forces prevent the sheet from drawing-in and may cause necking, but insufficient forces may lead to wrinkling (Fig. 2.19).
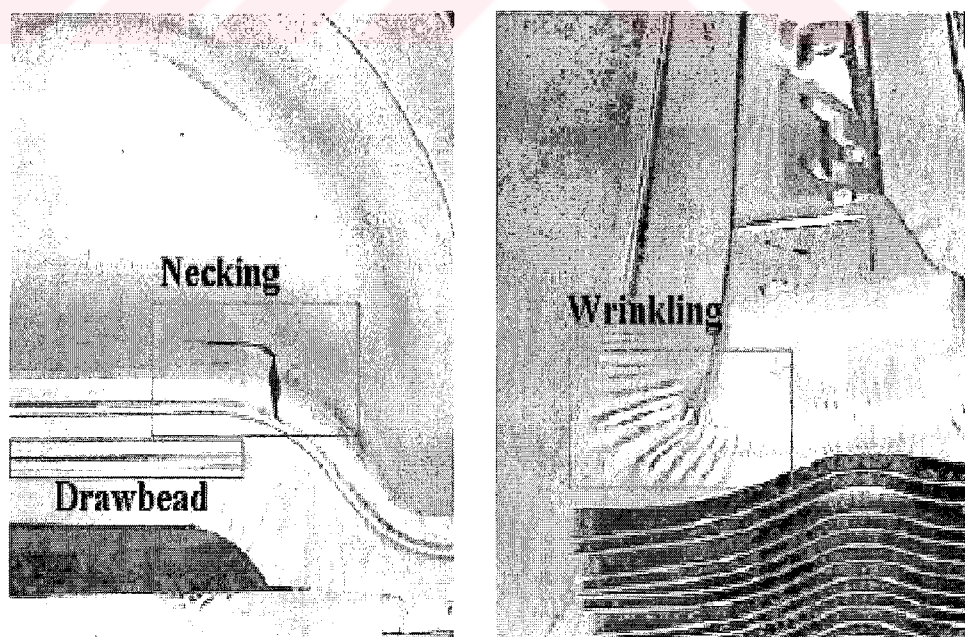
Fig. 2.19: Necking and Wrinkling Defects in the Forming Process.

The introduction of drawbeads in the mating tooling elements affects the level of tension that extends into the sidewalls of parts. Another important disadvantage of drawbeads is that they are difficult to adjust during die tryout and during production runs. In die tryout, adjustment is needed to obtain the proper restraining force. Once in production it would be desirable to allow adjustment for lot-to-lot variations in sheet metal yield strength and formability. This difficulty arises because changes in the drawbeads are made manually through hand grinding and welding [15].

In the view of computer simulation of parts, real drawbead geometries are seldom included, because that actual drawbead geometry modelling will lead to a large number of elements on the small radii of drawbeads and large computational time. In addition to this, the positions and shapes of drawbeads require several modifications during the forming tool design so that in the sheet forming simulation the drawbeads are often replaced by equivalent drawbeads which are defined as fixed lines on the tool surface.

3. MATHEMATICAL DRAWBEAD MODELS

Drawbeads are widely used in sheet metal forming processes to control the flow of sheet metal. To take into account the effects of the drawbead in the sheet metal forming process, the drawbead should be modelled properly in a finite element simulation to guarantee an accurate simulation. However, modelling the exact drawbead geometry requires a large number of elements due to the small radii of the drawbead. Evidently this large number of elements will increase the computation time for such finite element simulations drastically. Also, the time step must be strongly decreased to describe the sharp evolutions associated with the sequence of bending /unbending /reverse bending imposed tooling. An equivalent drawbead approach is therefore commonly adopted in finite element codes to overcome this problem of excessive computation time. The commonly used equivalent drawbead models represent the drawbead as an additional and constant drawbead restraining force and binder hold down force. The mathematical models represented in this thesis are Weidemann, Kluge and Stoughton, whereas the model of Stoughton is used most widely.

3.1 Simple Analytical Drawbead Model

The simple analytical models to determine the DBRF can provide a first insight into the performance of the drawbeads. Only DBRF can be calculated by this simple formula. In the simple analytical model, DBRF can be written as follow;

$$DBRF = f(K, R, t, n) \tag{3.1}$$

Where K: material strength

R: bending radius

t: sheet thickness

n: strain hardening exponent

In the simple analytical model, bending force or drawbead restraining force can be derived as follow [2].

A moment M per millimeter width is needed to bend a strip with thickness t along a radius R, see Figure 3.1.
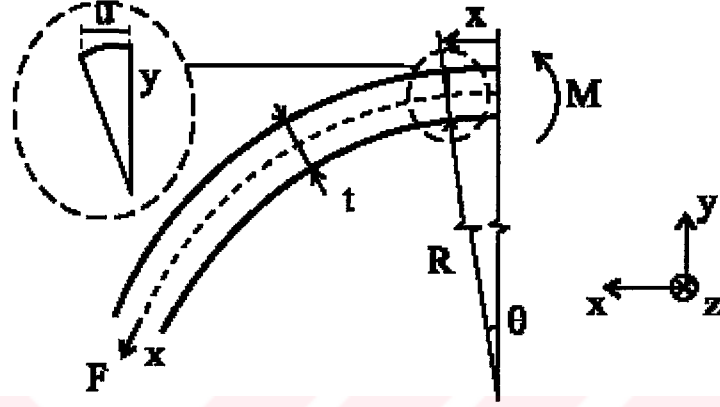
Figure 3.1: Principle Outline for Calculation of the Bending Force

Assuming a fully plastic moment and that the neutral plane coincides with the mid-plane, this moment can be written as:

$$M = 2 \int_{0}^{\frac{1}{2}t} \sigma_x y \, dy \qquad (3.2)$$

The material is assumed to obey both the Ludwik-Nadai hardening law and the Von Mises yield criterion. Hence, the stress in the plane strain situation can be written as:

$$\sigma_{ps} = \frac{2}{\sqrt{3}} K \varepsilon^n \quad \text{where} \quad \varepsilon = \frac{u}{x} = \frac{y\theta}{\left(R + \frac{1}{2}t\right)} \qquad (3.3)$$

Substitution of equation (3.3) into (3.2) gives:

$$M = \frac{4K}{\sqrt{3\left(R + \frac{1}{2}t\right)^n}} \frac{1}{(n+2)} \left(\frac{1}{2}t\right)^{n+2} \qquad (3.4)$$

22

The force needed to bend the strip can be calculated by equating the internal and external work. The internal work yields:

$$W_{int} = \int\int \sigma \varepsilon dA = \int\int \sigma \kappa y dA = 2\kappa \int_{0}^{\frac{1}{2}t} \int \sigma y \, dy \, dx = M\kappa\left(R + \frac{1}{2}t\right)\int_{0}^{\theta} d\alpha = M\theta \qquad (3.5)$$

Where curvature $\kappa = \dfrac{1}{\left(R + \dfrac{1}{2}t\right)}$ and strain $\varepsilon = \kappa y$

The external work is given by:

$$W_{ext} = Fx \qquad (3.6)$$

The drawbead restraining force (DBRF) per millimeter width can be calculated by equating equations (3.5) and (3.6).

$$F = DBRF = \frac{M\theta}{x} = \frac{4K}{\sqrt{3\left(R + \dfrac{1}{2}t\right)^{n}}} \frac{1}{(n+2)}\left(\frac{1}{2}t\right)^{n+2} \qquad (3.7)$$

Simple analytical model includes a number of simplifications; friction, sheet thinning, anisotropy, elastic deformation of the sheet material, the bead penetration and clearances and cavity in the drawbead geometries are not taken into account [2].

As a first orientation, this simple analytical model which includes a number of simplifications is compared with more sophisticated analytical model, Stoughton drawbead model.

Table 3.1: Semi-circular Drawbead Geometry (mm)

Semi-circular drawbead geometry (mm)	
Bead radius	8
Groove radii	5
Bead height	8
Clearance	1.1
Blank thickness	1.1

A specific drawbead geometry is chosen as shown in Table 3.1. The material model applied here has material strength (K), value of 577 MPa. Hardening exponent is

0.36, and friction is neglected. In this drawbead with a semicircular cross-section, the material will be bent and sequentially unbent two times around a radius of 5 mm and once around a radius of 8 mm. The results compared with Stoughton model are listed in Table 3.2

Table 3.2: The Comparison Result Between Simple And Stoughton Analytical Drawbead Models

	Simple model	Stoughton model without friction	Stoughton model with friction of 0.162
DBRF (kN/mm)	0.0684	0.0614	0.0855

It can be conculated that the simple analytical drawbead model to determine the DBRF can provide a first insight into the performance of the drawbeads.

3.2 Weidemann's Drawbead Model

In 1978, Weidemann proposed an equivalent drawbead model. He examined the blank holding action of drawbeads and derived a simple formula to calculate the drawbead restraining force as follow [1]:

$$
\begin{aligned}
DBRF = tw\Bigg\{ & \frac{2\mu P}{t}e^{4\mu\theta} + \frac{2\sigma_y t}{\sqrt{3}}\Bigg[\Bigg(\Bigg(\Bigg(\frac{e^{\mu\theta}}{4\left(R_g + \frac{1}{2}t\right)} + \\
& \frac{1}{4\left(R_g + \frac{1}{2}t\right)} + \frac{1}{4\left(R_b + \frac{1}{2}t\right)}\Bigg)e^{2\mu\theta} + \frac{1}{4\left(R_g + \frac{1}{2}t\right)} + \\
& \frac{1}{4\left(R_b + \frac{1}{2}t\right)}\Bigg)e^{\mu\theta}\Bigg] + \frac{1}{4\left(R_g + \frac{1}{2}t\right)}\Bigg\}
\end{aligned}
\tag{3.8}
$$

The drawbead restraining force (DBRF) in the Weidemann analytical model depends on the following parameters;

$$DBRF = f(t, w, \mu, P, \sigma y, \theta, Rg, Rb) \tag{3.9}$$

Where t: initial sheet thickness

w: sheet width (or bead length)

μ: coefficient of friction

P: effective blankholder force per unit length of the bead (the blankholder force is applied to the flat surface of the blank)

σy: yield stress

θ: bending angle of the blank

Rg: shoulder radius of the groove

Rb: bead radius

Weidemann's drawbead force model is simple in form, and it is convenient to use. However, it has the following shortcomings [1]:

1-The strain hardening of the sheet is ignored, and bending and unbending stress is assumed to be the same at each corner. However, the sheet strain hardens after every bending and unbending. Therefore, this assumption results in an underestimation of the drawbead restraining force (DBRF).

2-The anisotropy of the material is neglected.

3-The elastic deformation of the sheet is neglected. Thus, the elastic force is ignored which results in an underestimation of the DBRF.

4-The thinning of the sheet after each bend and unbend is neglected which results in an overestimation the DBRF.

5-The model calculates the drawbead restraining force (DBRF) but minimum binder hold down force (BHF) necessary to prevent the lifting-up of the binder still needs to be determined.

6-The bending angle needs to be determined.

7- For any bead penetration, the effective bending radius is assumed to be equal to bead or groove radius which would resulting an overestimation of the bending strain for shallow bead penetration.

3.3 Kluge's Drawbead Model

Kluges derived a drawbead restraining force model using an approach similar to that in Weidemann's work but introducing strain hardening into the model by calculating the average yield stres during each bending and unbending deformation. Kluge's formula to calculate the drawbead restraining force as follow [1]:

$$
DBRF = \left\{ \left[\left[\left(\mu F_N + \frac{\sigma_1 t^2 w}{4\left(R_g + \frac{1}{2}t\right)} \right) e^{\mu\theta} + \frac{\sigma_2 t^2 w}{4\left(R_g + \frac{1}{2}t\right)} + \right. \right. \right.
$$

$$
\left. \left. \frac{\sigma_3 t^2 w}{4\left(R_b + \frac{1}{2}t\right)} \right] e^{2\mu\theta} + \frac{\sigma_4 t^2 w}{4\left(R_b + \frac{1}{2}t\right)} + \frac{\sigma_5 t^2 w}{4\left(R_g + \frac{1}{2}t\right)} \right\} e^{\mu\theta} + \frac{\sigma_6 t^2 w}{4\left(R_g + \frac{1}{2}t\right)} + \mu F_N \quad (3.10)
$$

The drawbead restraining force (DBRF) in the Kluge analytical model depends on the following parameters;

$$
DBRF = f(t, w, m, F_N, \mu, n, \theta, Rg, Rb) \quad (3.11)
$$

Where t: initial sheet thickness

w: bead length

F_N: effective blankholder force

n: strain hardening exponent

μ: coefficient of friction

θ: bending angle

Rg: groove radius

Rb: bead radius

The structure of this model is very similar to Weidemann's model. However, it takes strain hardening into account by a piece-wise consideraion of the flow curve. The material anisotropy, the elastic force originating from the elastic deflection of the sheet, and the thinning of the sheet are neglected. For any bead penetration, the effective bending radius is assummed to be equal to the bead or groove radius. This would results results in an overestimation of the bending stres for shallow bead penetration [1].

The model can estimate the drawbead restraining force but the binde hold down (BHF) necessary to precent the lifting up of the binder while while the metal flows through the bead, still needs to be determined.

3.4 Stoughton Drawbead Model

A frequently used and more sophisticated analytical model to determine the drawbead force is proposed by Stoughton [Stoughton, 1988]. The drawbead model of Stoughton has been proved very satisfactory compared to others [30]. This model is based on the principle of virtual work: the work required to pull (or to restrain) a sheet through a drawbead is equal to the work required to overcome the sheet-tool friction and to bend or unbend the sheet. The Stoughton model makes use of the effective material bending radius instead of the drawbead radii. The material is assumed to obey the Holomon hardening law which incorporates strain rate sensitivity. This hardening law degenerates to the Ludwik-Nadai hardening law when strain rate effects are neglected [16].

The virtual plastic work due to the bending–unbending gives the restraining force Fi (per unit of length) at each point of radius change (Fig. 3.2):

$$F_i = \int\limits_{-t_i/2}^{+t_i/2} \left(\int\limits_{\varepsilon_i^-}^{\varepsilon_i^+} (\sigma.d\varepsilon) \right).dz \qquad (3.12)$$

where ti is the thickness, ε and σ are the strain and stress along the pull direction, ε_i^- and ε_i^+ are the strains before and after the with ith radius change.

For a semicircular drawbead, the number of bending and reverse bending deformations is six (Fig. 3.2). As a result, the total drawbead restraining force per unit length from the accumulation of bending and frictional forces from various regions of the semicircular drawbead is given below [1]:

$$DBRF = \left[\left(F_1 e^{\mu\theta} + \mu F_e + F_2 + F_3 \right) e^{2\mu\theta} + \mu F_e + F_4 + F_5 \right] e^{\mu\theta} + F_6 \qquad (3.13)$$
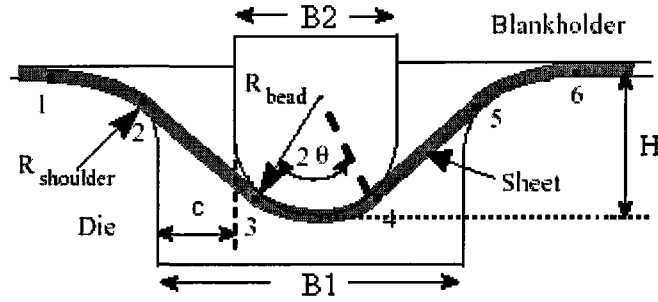
Figure 3.2: Drawbead Geometry with Bending–Unbending at 1–6

Complete formulation of Stoughton drawbead forces can be found in the reference [1]. The drawbead restraining force (DBRF) in the Stoughton analytical model depends on the following parameters;

$$DBRF = f(t_i, w, \mu, K, n, R_{eff}, r, \theta, E, m, \varepsilon, \varepsilon_i) \qquad (3.14)$$

Where t_i: current sheet thickness at the i-th bending or unbending point

w: sheet width (or bead length).

μ: coefficient of friction

K: material strength

n: strain hardening exponent

R_{eff}: effective bending radius

r : normal anisotropy coefficient

θ: bending angle

E: Young's modulus

m: strain rate exponent

$\dot{\varepsilon}$: strain rate

ε_i current strain at the i-th bending or unbending point (see Figure 3.2)

The structure of this model is more complex than the other two models but it has the following advantages:

1-The strain hardening of the sheet is taken into account.

2-The anisotropy of the material is taken into account.

3-The elastic deformation of the sheet is taken into account.

4-The thinning of the sheet after each bend and unbend is taken into account.

5-The model calculates both the drawbead restraining force (DBRF) and the binder hold down force (BHF).

6-The bending angle is calculated.

7-The effective bending radius is calculated due to the bending angle [3].

There is an important point when we consider Stoughton analytical drawbead model. If the clearance between the groove and the bead (c=B1-B2, see Figure 3.2 and 3.3) is narrow and equals the blank thickness. This means that the blank is forced to mainly follow the drawbead geometry, see Figure 3.3a. Note that for clarity only the mid-plane of the deformed blank is plotted. The analytical Stoughton model is based on this type of deformation patterns and hence the agreement between the analytical results and the simulation results will be good.

a)   b)
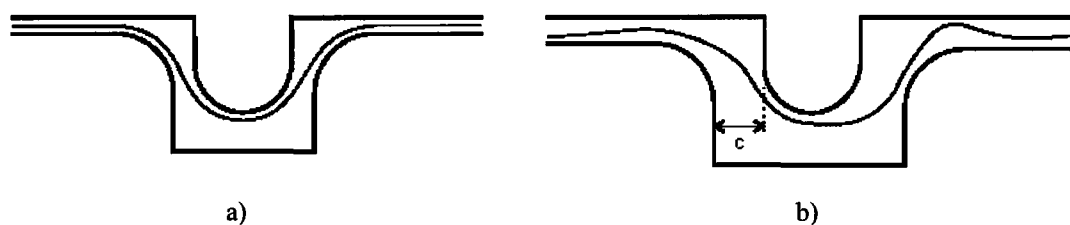
Figure 3.3: Deformed Blank in Different Drawbeads

However, if the clearance between the groove and the bead is larger than the blank thickness, as a result the deformed blank shape will look like Figure 3.3b. The analytical Stoughton model is not able to deal accurately with this type of deformation pattern, which leads the larger deviation between the analytical and the experimental drawbead forces [2].

The mathematical models represented in this thesis have identified the relationship between the drawbead forces and drawbead geometry. However, all the observations assume that the sheet metal matches the drawbead geometry while it is pulled through the drawbead. Yellup and Painter observed (through photographs) that for shallow bead penetrations the strip did not wrap tangentially around the bead while it was pulled through the drawbead. Green expanded on the work done by Yellup and Painter to experimentally determine the behaviour of the sheet metal strip as it moves through a drawbead. Green observed that bead penetration had an effect on the amount of bead wrap. At shallow penetrations, the strip contacts the bead at only one point. As penetration increases, the wrap angle also increases. Finally, at very deep penetration, the "full bead wrap" assumption becomes valid [17].

4. EFFECTS OF PARAMETERS ON DRAWBEAD FORCES

Drawbead design and drawbead force control are essential in sheet metal design and forming good quality sheet metal components. Drawbead forces are related to the drawbead geometry (shape and dimension), sheet material (thickness and mechanical properties) and process parameters.

Without extensive knowledge of the influences of all these variables on the drawbead forces, it is hardly possible to design the drawbead geometry adequately to manufacture a product with the desired shape and performance. This section investigates the effects of sheet thickness, material properties and drawbead geometry on the drawbead forces.
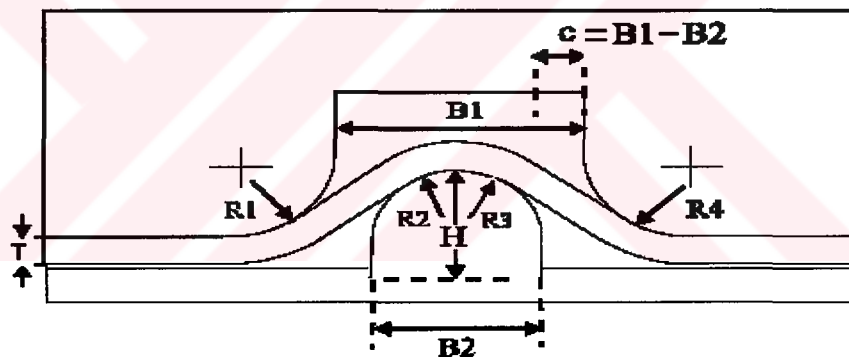
Figure 4.1: Drawbead Geometry with Semi-circular Cross Section

The height, shape, and size of a drawbead governs the amount of restrictive force generated. A sharp drawbead radii decrease metal flow, while a large drawbead radii allow material to flow more freely. The parameters effected on drawbead forces as follows :

1-The geometry of drawbead, see Figure 4.1

    clearance, c = B2-B1

    bead penetration, H

    bead radius, R2 and R3

grove radius, R1 and R4

length and width of drawbead

2-Sheet Metarial Properties

sheet thickness

elastic properties

stres-strain relation

anisotropy of sheet material

3-Proses parameters

drawing speed

coeficient of friction

blankholder force

Using the Stoughton's drawbead model in Pam Stamp 2G v2004, the calculations are performed to investigate the effects of the parameters on the drawbead forces. The results are given in Figure 4.2 to Figure 4.7.
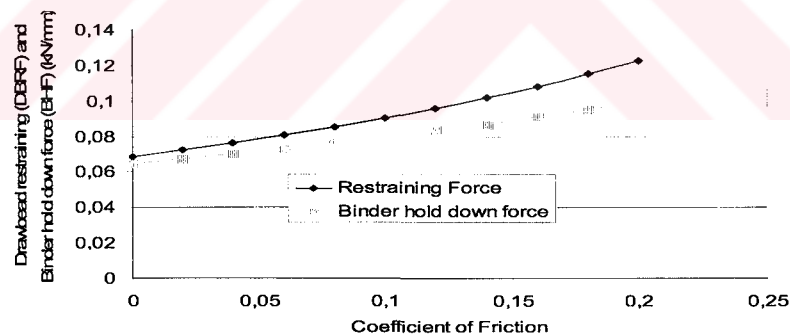
Figure 4.2: The Drawbead Forces as a Function of Coefficient of Friction

Figure 4.3: The Drawbead Forces as a Function of Bead Penetration (The Height of Bead)

The height of the bead or penetration of bead, up to the point where the bending/unbending ceases to have its maximum effect, has the greatest influence on the degree of material control. Penetration of bead affects the bending (and unbending) angle and radius. For shallow penetrations the effective (actual) bending radius of the sheet is greater than the radius of the bead or groove, and hence, the bending and unbendin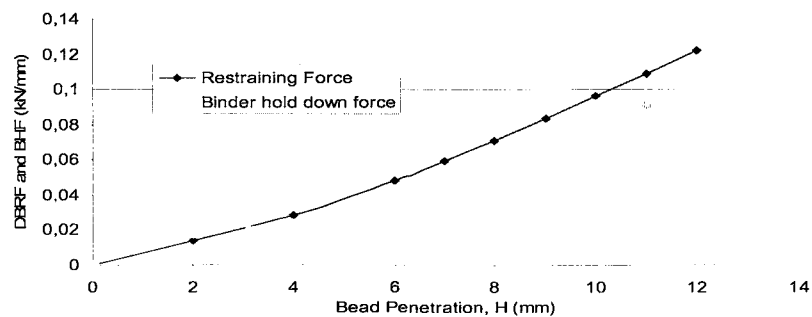g stress is lover. Also the bending/unbending angle is smaller, and hence, the coil friction force, which depends on the winding angle, is low [18].

Figure 4.2 and 4.3 show the relation between the drawbead forces and coefficient of friction and the bead penetration respectively. When the bead penetration increases, the deformation range in the blank increases and so does the covering angle over which the plate acts on the bead. As a result, the bending and unbending deformation around the drawbead and coil friction increases which leads to the increase in the drawbead forces.

It can be concluded that the drawbead forces are affected mainly by bending and unbending deformations, therefore increasing the total number of the bends and unbends by using rectangular or multiple beads will increase the total bends. Experimental observations have shown that [19]:

i. increasing bead penetration increases the drawbead forces,

ii. increasing bead penetration causes more surface damage,

iii. increasing bead penetration increases the final sheet hardness.

iv. increasing drawing speed decreases the drawbead restraining force (DBRF),

v. decreasing drawing speed increases surface damage,

vi. decreasing lubricant efficiency increases the drawbead forces,

vii. decreasing lubricant efficiency increases surface damage.

A variable drawbead forces, as an alternative to the blankholder force control, may be an efficient and cost effective way to control drawing operations. With a mechanically or hydraulically driven unit, it may be possible to develop a control strategy to adjust the drawbead forces in space (locally) and in time by changing the bead penetration during the process so that the tearing and wrinkling of the sheet metal can be prevented (see Section 2, page 17).
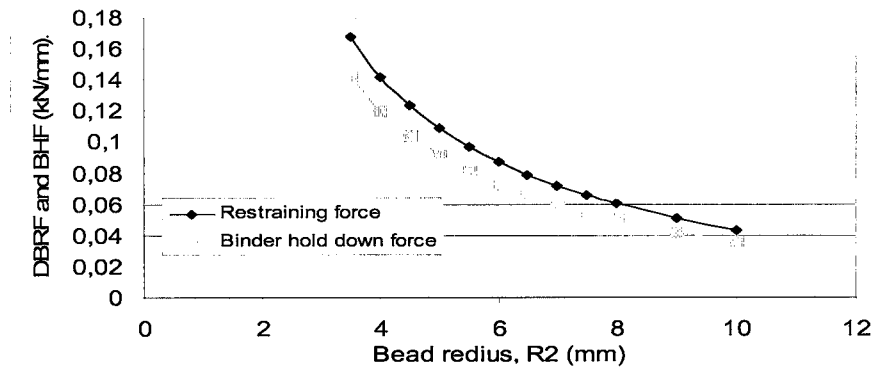
Figure 4.4: The Drawbead Forces as a Function of Bead Radius
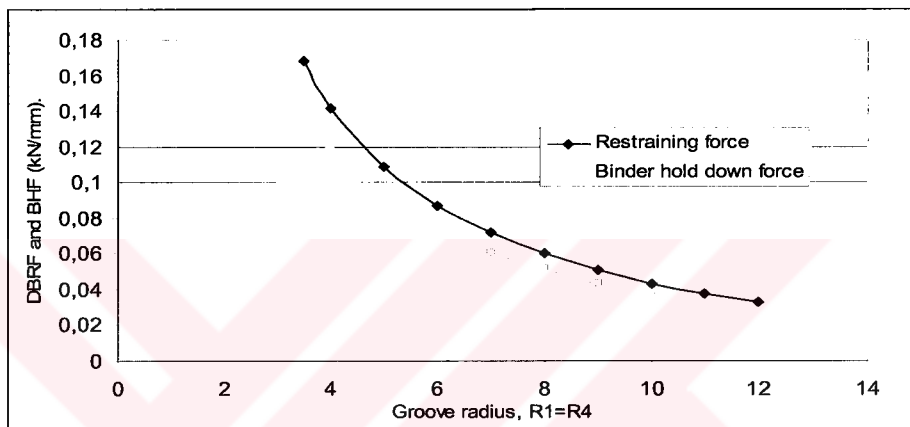
Figure 4.5: The Drawbead Forces as a Function of Groove Radius

Figure 4.4 and 4.5 show the relation of the drawbead forces via the radius of the bead and that of the groove shoulder, respectively. It can be seen that the resistance decreases as the radius of the drawbead increases. Decreasing bead or groove radius increases the drawbead forces linearly, or vice versa. When the drawbead radius increases, the bending and unbending deformation of the plate decreases as it passes through the drawbead, which results in a decrease in the drawbead forces.
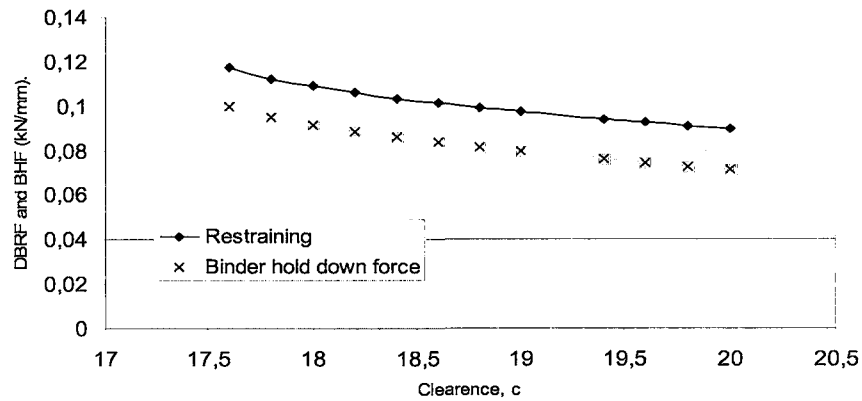
Figure 4.6: The Drawbead Forces as a Function of Clearance
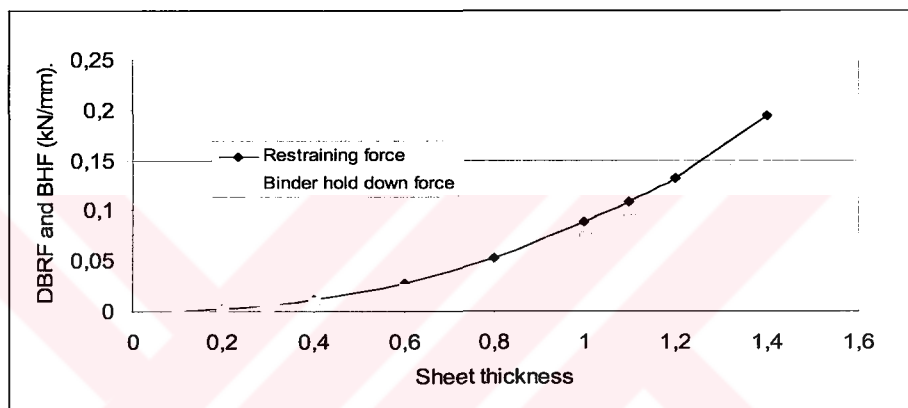
Figure 4.7: The Drawbead Forces as a Function of Sheet Thickness

According to Figure from 4.4 to 4.6, it is clear that the influence of drawbead height, drawbead radius and groove shoulder radius on the drawbead forces is very great. Therefore, the most effective way to control the drawbead forces in practice is to adjust these three parameters. In Figure 4.7, increasing sheet thickness increases the drawbead forces linearly.

It can be seen from the results that both the restraining and the binder hold down force are related to the blank material and the bead geometry parameters. For a certain blank, the bead radius (R_b), the groove shoulder radius (R_g) and the bead height (H) are the key factors influencing the restraining force. Within these parameter bead penetration has the greatest influence on the drawbead forces. The effects of drawbead parameters which are mentioned above are tabulated in Table 4.1.

Table 4.1: Changes in the Restraining Forces with the Parameters

Coefficient of Friction (μ)	Bead Penetration (H)	Bead Radius (R_2)	Groove Radius (R_1, R_4)	Clearance (c)	Thickness (t)	Drawbead Forces (DBRF, BHF)
↗	Constant	Constant	Constant	Constant	Constant	↗
Constant	↗	Constant	Constant	Constant	Constant	↗
Constant	Constant	↗	Constant	Constant	Constant	↘
Constant	Constant	Constant	↗	Constant	Constant	↘
Constant	Constant	Constant	Constant	↗	Constant	↘
Constant	Constant	Constant	Constant	Constant	↗	↗ ↗

It should be noted that in sheet metal forming due to the metal flow, the sheet metal gets thicker or thinner and strain hardens before it flows into the drawbead. Therefore, the drawbead forces may be different from the predicted value due to the level of thickness change and strain hardening. Secondly, if blankholder force is applied on the flat portion of the sheet, it not only creates a friction resistance force between the sheet and the binder surface but also stretches the sheet in the drawbead which would create an additional frictional resistance between the sheet and the groove/bead shoulders. Therefore, the drawbead restraining and the binder hold down forces increase superficially. However, this makes the process hard to control.

5. ESTIMATION OF DRAWBEAD FORCES

An accurate information on drawbead forces are indispensable for sheet forming design and finite element modelling. To design and implement drawbead forces in forming processes, it is necessary to know the drawbead restraining force (DBRF) and binder hold down force (BHF).

This part of the thesis deals with the drawbead behaviour. In order to get more insight in the drawbead behaviour a number of numerical analyses were performed. These analyses give the information on the drawbead forces. To verify these analyses, the results obtained by numerical simulations are compared with experimental results.

5.1 Experimental Results

In this part, experimental results in literature [20] are used to validate the performance of drawbeads. A principle outline of this experimental setup is given in Figure 5.1 and 5.3. Complete specifications and dimensions of the drawbead are shown in Figure 5.2.
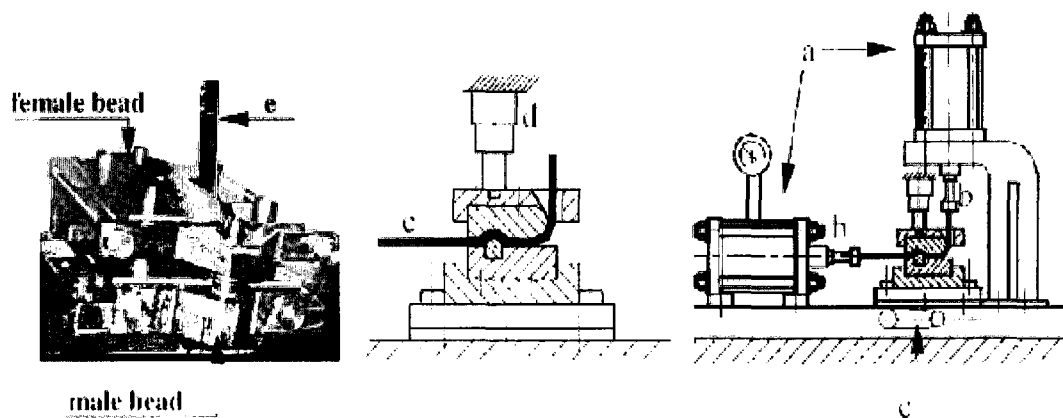
Figure 5.1: Experimental Setup of the Drawbead Tester: (a) Hydraulic Cylinders; (b) Load Cells; (c) Pressure Regulator Valve; (d) Transducer; (e) Test Strip.

Dimensions (mm)							
FEMALE BEAD	b	r˟	h˟	B	R˟	H	L
SQUARE	16	3	11	18	5	13	55
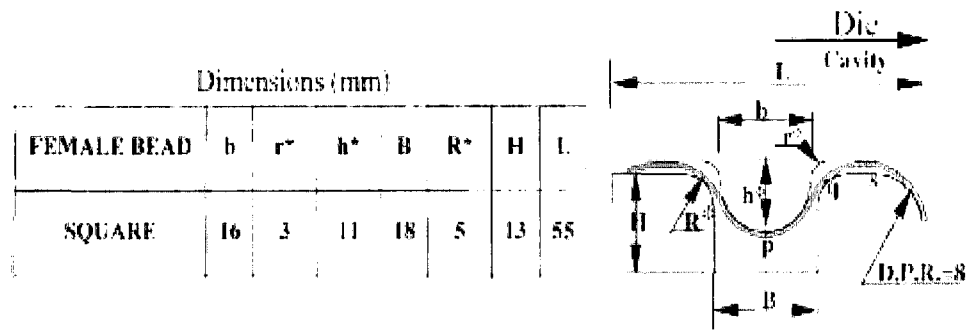
Figure 5.2: Complete Specifications and Dimensions of the Drawbead

The material considered in this experiment is the aluminium alloy of thickness 1.1 mm. The mechanical properties of this material are given in Table 5.1. The strip size is 40 mm wide and 160 mm long. The nominal punching and pulling velocity are 20 mm/min. The friction coefficient for the experiment is obtained 0.162 [20].

Table 5.1: Material Properties of the Strip

Properties	Value
Yield Stress (GPa)	0.136
Young's Modulus (GPa)	71
Plastic anisotropy parameter, r	0.64
Work-hardening exponent	0.36
Coulomb friction coefficient	0.162
Strength coefficient (GPa)	0.577
Poisson's ratio	0.33
Initial elastic strain component	0.0166
Thickness (mm)	1.1
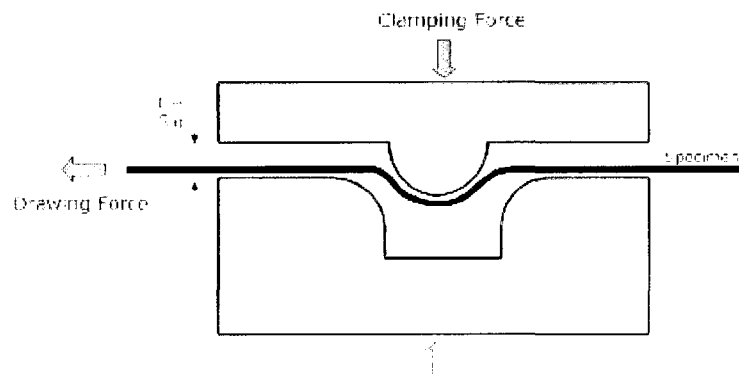
Figure 5.3: Die Shape and Dimensions for the Drawbead Test.

In the experimental test, a strip of sheet material is clamped between a blankholder and a die as shown in Figure 5.3. The drawbead is situated in the blankholder-die region. The material is pulled through the drawbead by moving the punch into the die cavity.
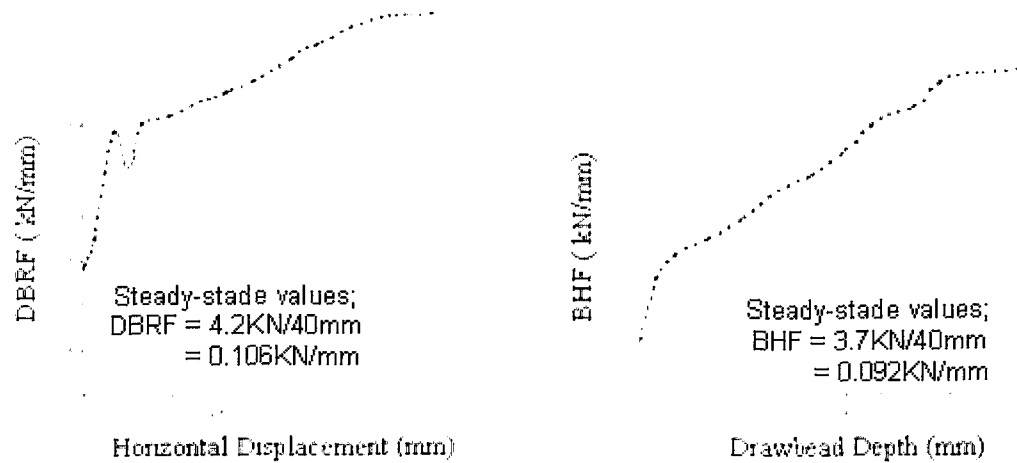
Figure 5.4: Experimental Drawbead Forces as a Function of Displacement

From Figure 5.4, it is seen that the steady-state values of drawbead restraining force (DBRF) and binder hold down force (BHF) are 0.1062 and 0.0925 kN/mm, respectively. In the next subject, these experimental values will be compared with numerical results in order to verify the reliability of the numerical models which can be used to determine the process dependent drawbead forces for all possible drawbead geometries.

5.2 Numerical Approaches

The physical mechanisms of forming processes like deep drawing are highly complex due to the non-linear behaviour of elasto-plasticity theory leading to a complex interaction of sophisticated product geometries in three dimensions and with respect to time. Theoretical descriptions for a better understanding are difficult as the sub-mechanisms can often not be separated or localized. However, proper product design, tolerances and quality demand for suitable tool development, corresponding to high costs and large lead times. Therefore in the field of sheet metal forming numerical simulation tools usually based on the Finite Element Method

(FEM), have become more and more common in the development process. They enable to predict how the press tools and parameters should be designed to achieve the optimum shape of the sheet metal components, thus substantially reducing the number of experimental trials. During this period of time the precision of the simulation tools has increased.

Numerical simulations considered in this thesis will be based on the finite element method. Three FE models are presented to simulate the drawbead behaviours; 3D plane stress drawbead model, 2D plane strain drawbead model and the equivalent drawbead model in which the real drawbead geometry replaces by a line on the tool surface on which a numerical algorithm acts. Numerical simulation were carried out via two commercial FEA software codes, namely Pam-Stamp 2G and Abaqus Standard.

5.2.1 3D plane-stress drawbead modelling

A 3D plane stress drawbead model is developed to obtain accurate data concerning the drawbead forces during the forming process. First, the reliability of the 3D drawbead model must be proven. Subsequently the model can be used to determine the process dependent drawbead forces for all possible drawbead geometries.

The simulation program that has been used in this investigation is Pam Stamp 2G v2004 which is an explicit FEM-code based on a central difference integration scheme. The sheet is modeled with four node bi-linear plane stress elements. The element type used is Belytschko-Tsay with 5 integration points through the thickness. The material model used is Hill48 with isotropic hardening.
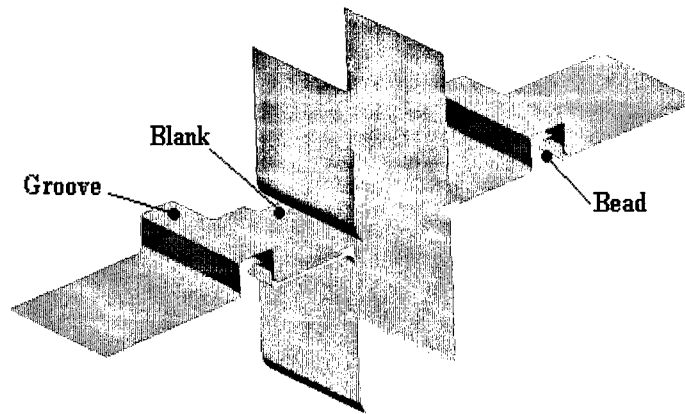
Figure 5.5: Finite Element Model of the 3D Plane Stress Drawbead Model.

The type and dimensions of the drawbead used in the simulations and the material properties are chosen as in the experimental study (see Figure 5.2). The finite element model is depicted in Figure 5.5. During the forming operation, the adaptive mesh algorithm is used, so initially 400 quadreteral elements are employed in the strip. The results obtained with the 3D drawbead model are given in Figure 5.6 and 5.7.

Horizontal displacement (mm)
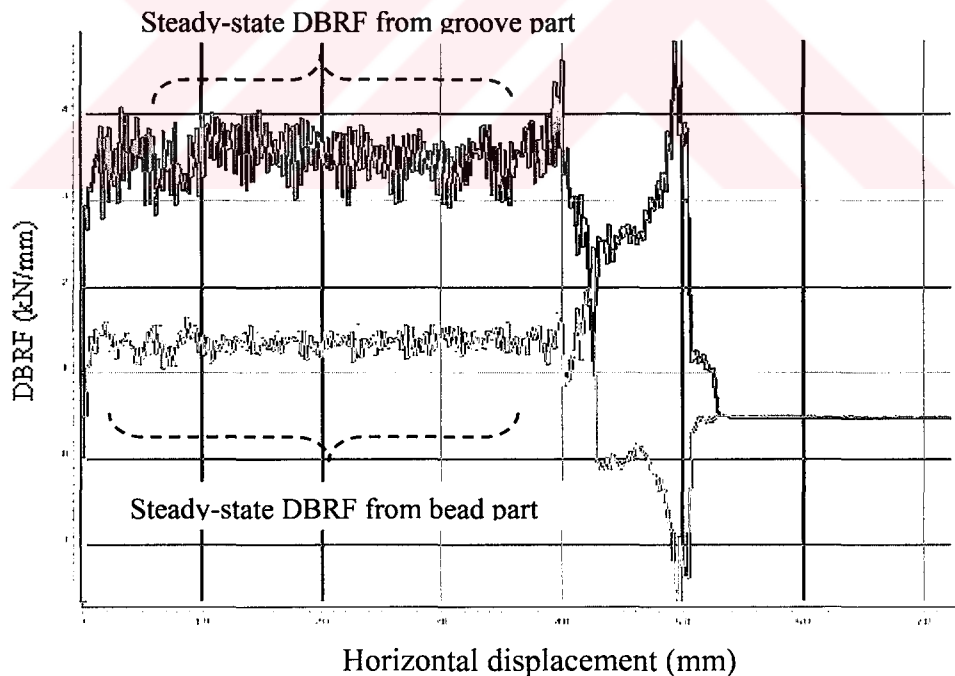
Figure 5.6: Drawbead Restraining Force (DBRF) Versus Displacement

Steady-state values of the DBRF at the groove part is 0.083 kN/mm (3.4 kN/40mm) and 0.03 kN/mm (1.2 kN/40mm) at the bead part. The total steady-state DBRF is 0.113 kN/mm.
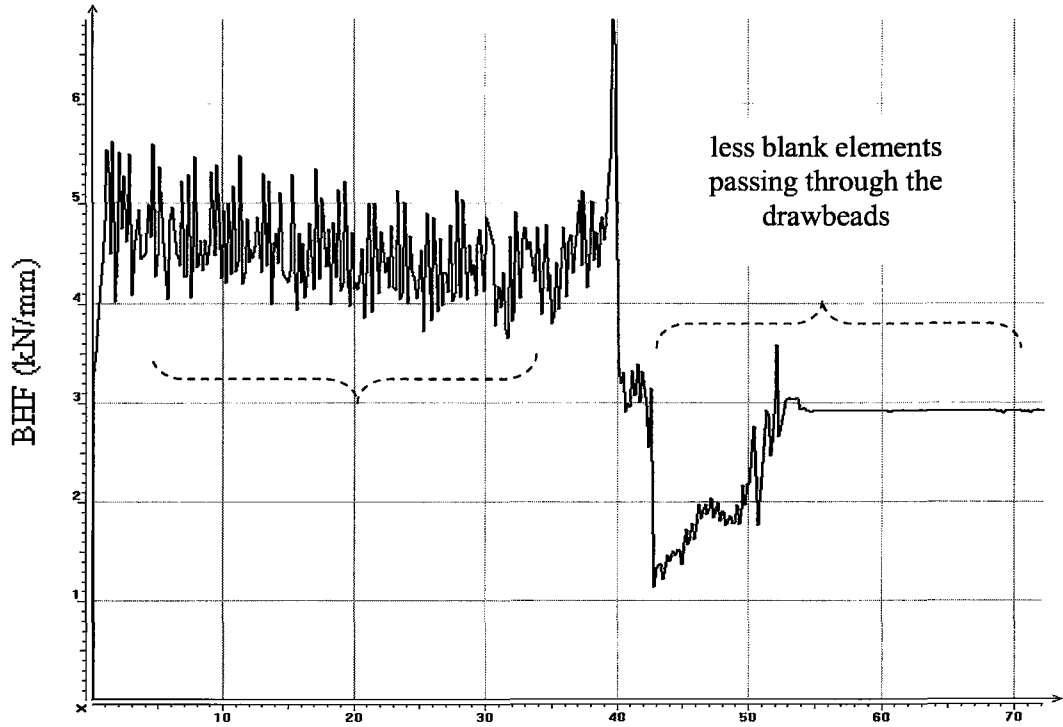
Figure 5.7: Binder Hold Down Force (BHF) Versus Displacement

The drawbead restraining force, DBRF is a distributed force along the drawbead line (kN/mm). It can be seen in Figure 5.5 and 5.6 that the steady-state value of the DBRF and the BHF are 0.115 kN/mm and 0.112 kN/mm, respectively. It can be said that these results can be converged much more than as the mesh density is increased. The agreement with the experiment is very good. Therefore it can be concluded that 3D plane stress model works very satisfactory to study the drawbead behaviour and this means that the reliability of the 3D drawbead model as a reliable tool to predict the drawbead forces is proven. Subsequently the model can used to determine the process dependent drawbead forces for all possible drawbead geometries.

5.2.2 2D Plane-Strain Drawbead Modelling

The analysis of metal flow along a drawbead, and the determination of the forces exerted by the tooling are generally performed under the assumption of plane strain condition. Apart from the advantage of simplicity, this choice is validated by the fact that drawbeads are often located at the border of long and fairly straight parts of the blank, for instance in the case of large and shallow automotive panels.

In this study, a 2D plane strain drawbead model is developed to obtain accurate data concerning the drawbead forces during the forming process. First the reliability of the 2D drawbead model must be proven as in the plane stress modelling. Subsequently the model can be used to determine the process dependent drawbead forces for all possible drawbead geometries.

The analysis is carried out using the commercial code namely Abaqus/Standard. Plane-strain conditions are assumed. The tools are defined by rigid surfaces. The numerical tool description for the 2D drawbead model is given as an exploded view in Figure 5.8. The profile of the sheet is modelled with quadrangular plane-strain elements. The number of elements in thickness direction is four and the total number of elements in the strip is 1708.
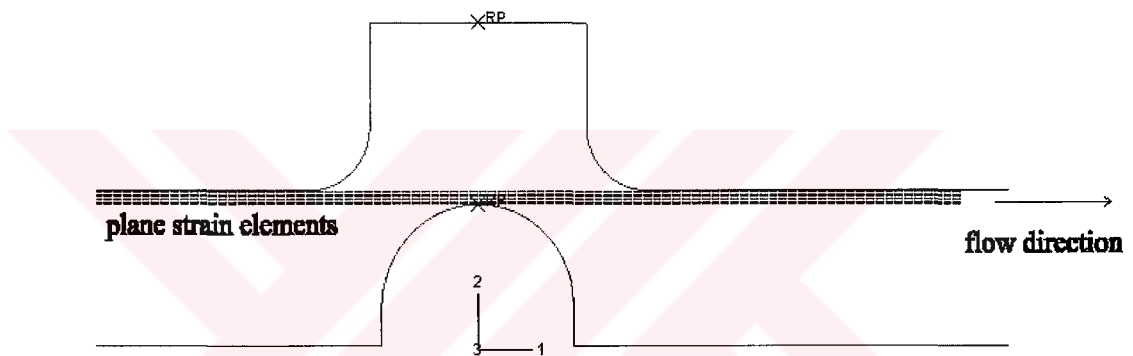
Figure 5.8: Finite Element Mesh of the 2D Plane Strain Drawbead Model.

Regular 4-node bilinear elements, denoted CPE4 in Abaqus, and elements with incompatible modes, denoted CPE4I, gave widely different results. In particular, exeedingly high values of the restraining force are obtained with elements CPE4, in comparison with results from the literature. Elements CPE4I are designed to avoid artificial stiffening due to parasitic shear stresses observed in bending with elements of type CPE4 [21]. In addition to this 8-node reduce integration plane-strain elements, denoted CPE8R provide substantially the same results as the CPE4I elements. Consequently, elements CPE4I are finally selected for the simulation. The mesh of the model and deformation steps are depicted in Figure 5.9.
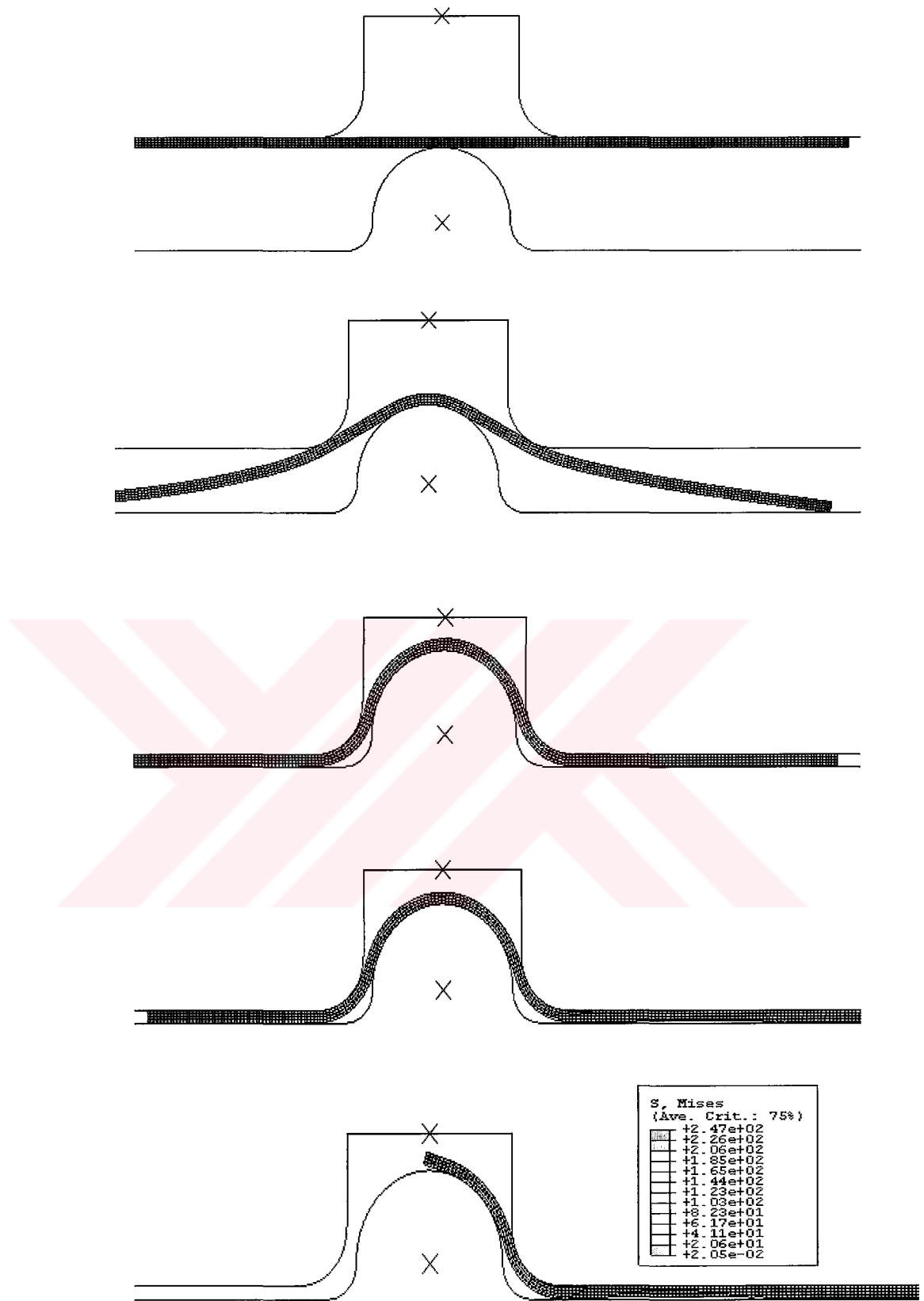
Figure 5.9: The Deformed Shape of the Drawbead Forming Process in the 2D Plane Strain Drawbead Model.
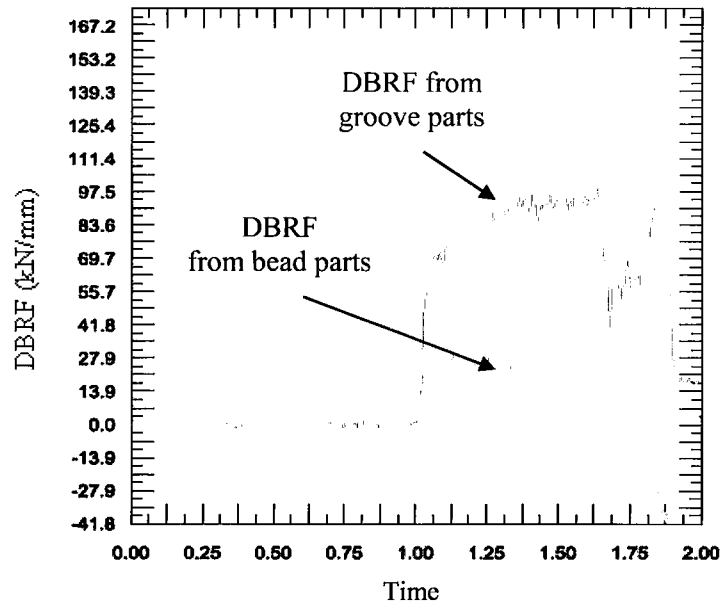
Figure 5.10: Drawbead Restraining Force (DBRF) Versus Time
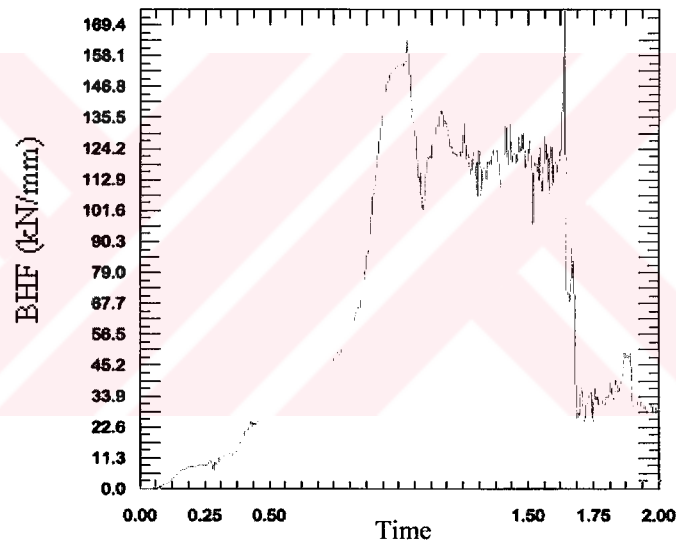
Figure 5.11: Binder Hold Down Force (BHF) Versus Time

It is seen from Figure 5.10 and 5.11, the steady-state value of the DBRF and the BHF are 0.120 kN/mm and 0.125 kN/mm, respectively. It can be said that this results can be converged much more than as the mesh density is increased. As a result, the 2D plane strain model works very satisfactory to study the drawbead behaviour. So we have a reliable tool to predict the drawbead forces for a given drawbead geometry.

Note that in the 2D plane strain drawbead model is based on a plane strain assumption. The plane strain assumption holds for the straight part of the drawbead.

If the drawbead is sufficiently long, the deformation pattern in the straight part of the drawbead can be assumed as plane strain. For this part of the drawbead, the real drawbead geometry can successfully be replaced by the equivalent drawbead model. However, the deformation pattern of the blank in the vicinity of the drawbead ends is fully three-dimensional and hence the plane strain assumption does not hold for these parts of the drawbead [22]. Improper design of the drawbead ends can cause the sheet to wrinkle and this phenomenon cannot be taken into account in the 2D plane strain drawbead model and the equivalent drawbead model.

5.2.3 Equivalent drawbead modelling

There are two different fashions in the simulation of the drawbeads. One way is to model the exact geometry of the drawbead. The blank will be subject to bending/unbending and friction forces when it slides through the drawbead. This involves a relatively fine meshing of the blank near to the bead with potentially high cost in computer time.

The second way is to set-up an equivalent drawbead model, in which the actual drawbead is replaced by its projection onto the binder surface, i.e. a flat surface that has the same width as the actual drawbead, a regular mesh being constructed for the flat surface. The restraining force produced by the actual drawbead is assigned to the nodes in the regular mesh of the equivalent drawbead following the virtual work principle. The sheet metal passing through the equivalent drawbead model is then subjected to the same restraining force as that produced by the actual drawbead. The use of an equivalent drawbead model avoids the need for using an extremely fine mesh for the sheet metal and, in consequence, a huge saving of computation time can be achieved without significant loss of accuracy. Furthermore, the equivalent drawbead model has more advantages compared to the use of the real drawbead geometry. The equivalent drawbead is a flexible design tool. The effect of varying the position or geometry of the drawbead on the material flow can be studied very easily without the necessity to adapt the CAD drawings for a variation in the position or geometry of the drawbead [2].

The equivalent drawbead model, represented as a line on the tool surface, is given in Figure 5.12. During the deep drawing simulation a finite element which passes the drawbead line will obtain an additional DBRF and a plastic thickness strain whilst the lift force is substracted simultaneously from the total blankholder force.

3D drawbead geometry   Equivalent drawbead
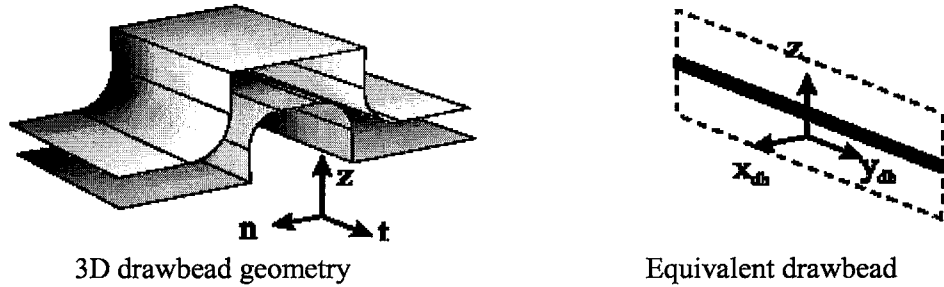
Figure 5.12: Schematic Drawing of a 3-Dimensional Drawbead and Its Equivalent Drawbead Representation

The material flow in the normal direction n only causes a DBRF and plastic thickness strain whilst the tangential component t makes no contribution, see Figure 5.12 [2]. This supports the approach to separate the total material flow into a normal and a tangential component. The coordinate system for the equivalent drawbead model is also given in Figure 5.12, where xdb and ydb denote the directions normal and tangential to the drawbead, respectively.

Based on the Stoughton's drawbead model, analytical calculations in PamStamp 2G v2004 software are made for the same conditions as those used for the experimental study as in the Section 5.1, we obtain the values of DBRF and BHF are 0.109 kN/mm and 0.0921 kN/mm respectively.

Table 5.2: Summary of Drawbead Force Estimation

Drawbead force estimation method	DBRF (kN/mm)	BHF (kN/mm)
Experimental	0.1062	0.0925
3D plane stress drawbead model (using PamStamp2G)	0.1130	0.1120
2D plane strain drawbead model (using Abaqus Standard)	0.1200	0.1250
Equivalent drawbead model (based on Stoughton model by using PamStamp2G v2004.1)	0.1090	0.0921
Equivalent drawbead model (using AutoForm 4.0)	0.1144	0.1254

In the Table 5.2, it can be seen that the results from numerical methods are very similar with the experimental results and give reliable predictions of the drawbead forces. The good agreement between the results shows that the equivalent drawbead model is a powerful tool to replace the real drawbead geometry in sheet metal forming simulations.

6. APPLICATIONS

Rapid developments in computer hardware make the finite element analysis of complex deformation responses increasingly applicable. The finite element method is used worldwide to simulate the sheet metal forming process and has become a reliable numerical simulation technology. For an accurate simulation of a real-life sheet metal forming process an accurate numerical description of the tools is necessary, as well as an accurate description of material behavior, contact behavior and other process variables.

Developments have been made in the field of finite element types, mesh adaptivity, material laws, failure criteria, wrinkling and surface defects, springback, contact algorithms, friction, simulation of new processes (for example hydroforming), optimization, process design and new analysis technique such as equivalent drawbead modelling.

In finite element simulations of the sheet metal forming process the drawbead geometries are seldom included because of the small radii. These small radii require a very large number of elements and therefore large computer time. In addition to this, working with real drawbead geometry is not flexible and suitable way in the case of finding optimum position and geometrical parameters of drawbeads on the material flow. It requires to adapt the CAD drawings. For these reason equivalent drawbead models which is representation of real drawbead geometry by a line on the tool surface on which a numerical algorithm acts are used. The effect of varying the position or geometry of the drawbead on the material flow can be studied very easily without the necessity to adapt the CAD drawings.

A principle goal of this section is to put forward the methodologies to obtain the accuracy of equivalent drawbead modelling technique and accurate prediction of drawbead behaviour on stamped part by using of the finite element method (FEM).

Five numerical models which are related to two separate geometries are developed and simulations are performed using the Pam Stamp 2G version 2004 finite element software.

6.1 Rectangular Product

Simulations are carried out to demonstrate the performance of the equivalent drawbead model in the forming analysis of a rectangular product. The numerical tool description for the rectangular product is given as an exploded view in Figure 6.1.
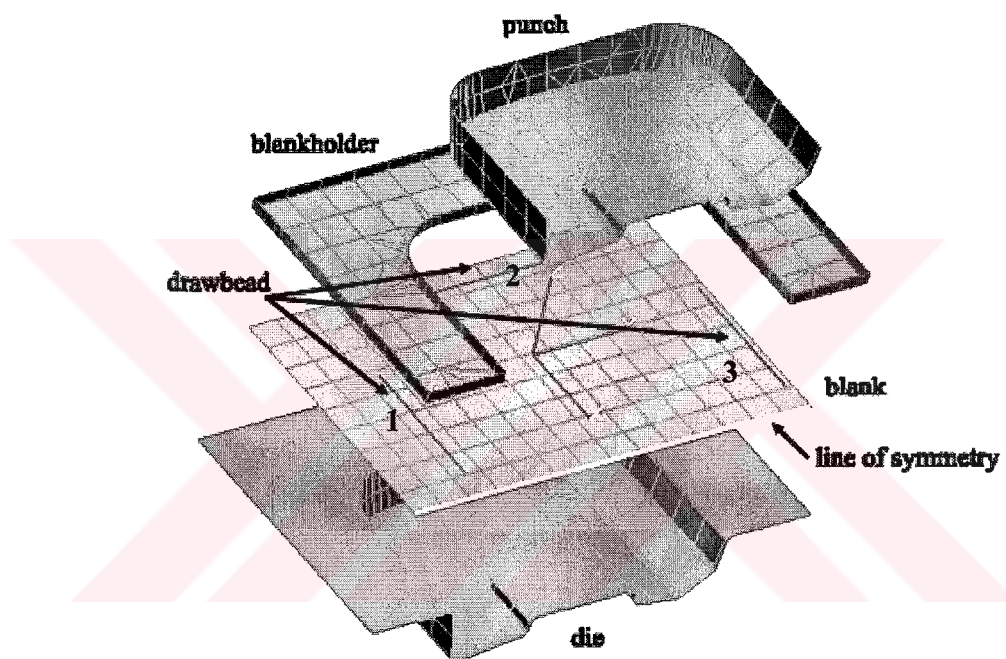
Figure 6.1: Exploded View of the Finite Element Mesh Used for the Symmetric Rectangular Product.

The tool geometry of the rectangular product comprises three equivalent drawbeads as a line located in the die-blankholder region as shown in Figure 6.1. The geometries of the drawbeads are equal and have total length of 400 mm. The drawbead characteristics are determined by using Stoughton's model; the restraining force sets 0.035 kN/mm and binder hold down force sets 0.05 kN/mm [23]. During the forming stage, blankholder force is defined constant value of 50 kN.

The adaptive meshing (mesh refinement) was used for the blank during the forming. The adaptive meshing automatically refines a mesh (that of the blank), where and

when it is required, so that the geometry is respected. This allows the coarsely meshed blank to be refined only as necessary during the simulation, minimizing the computational effort. The refined finite element mesh of the blank before and after the forming is shown in the Figure 6.2.

A-initial mesh   b-final mesh
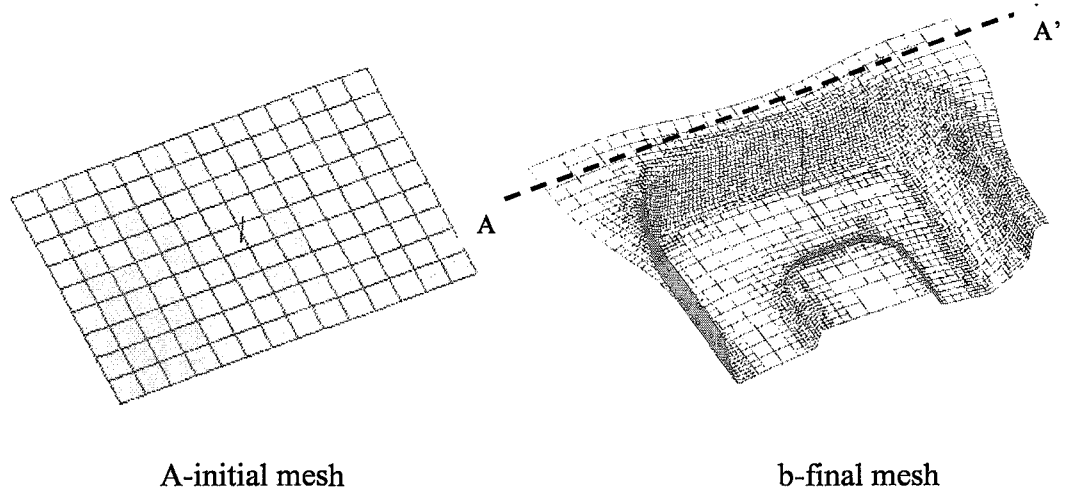
Figure 6.2: The Refined Finite Element Mesh of the Blank

Before the forming simulation, initial blank mesh has 150 elements, and at the end of the forming stage the total elements are 5785. Contact between the sheet and the tools are described with contact elements in which a friction coefficient of 0.12 is assumed. In the calculation the tool geometries are meshed as non-deformable rigid elements. They are the set of non elasto-plastic elements in which no strain is applied. The material used in this simulation is shown in Table 6.1 [23].

Table 6.1: Material Properties for the Rectangular Product

Properties	Value
Yield Stress (GPa)	0.135
Young's Modulus (GPa)	210
Plastic anisotropy parameter, r0	1.33
Plastic anisotropy parameter, r45	1.36
Plastic anisotropy parameter, r90	1.69
Work-hardening exponent	0.22
Coulomb friction coefficient	0.12
Strength coefficient (GPa)	0.52
Poisson's ratio	0.3
Thickness (mm)	0.5

Using the PamStamp2G software, two elasto-plastic explicit finite element simulations are performed. One simulation is performed in which the equivalent drawbead model was applied and the other one is carried out without drawbeads. The geometry and loading are symmetric, so in the simulation only half of the rectangular product is taken into account. The discussion of the results obtained will be on the differences between the simulations with and without the equivalent drawbead model.

Figure 6.3 shows the thinning distribution in the symmetric rectangular product for both cases. It was observed that excessive thinning regions are increased in the product with drawbeads which is also expected because the drawbead obstruct the flow of material.

With drawbead   **without drawbead**
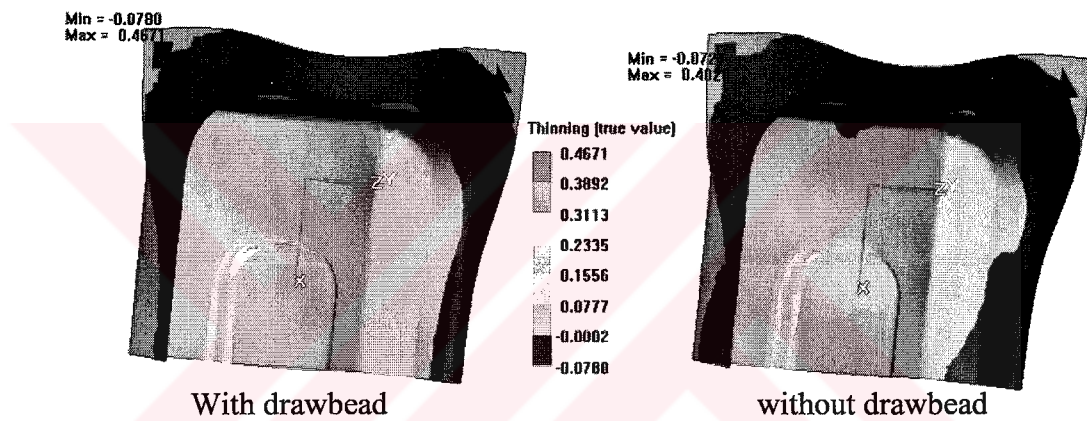
Figure 6.3: Thinning Distribution in the Symmetric Rectangular Product

The drawbead restraining force should be locally reduced where the sheet metal cannot easily flow into the die cavity. As a result, the value of restraining force caused from the drawbead 2 (see Figure 6.2) can be reduced.

At the final stage of the forming, the equivalent plastic strain distribution at the final stage of the forming in the symmetric rectangular product for both cases is given in Figure 6.4. The maximum plastic strain in the product with drawbeads is 0.5906 whereas the maximum plastic strain in the other simulation carried out without drawbeads is 0.4753. This figure clearly shows that the strain distribution in the rectangular product changes due to the applied drawbeads. Roughly, the plastic strain in the rectangular product is increased by 0.11 when the equivalent drawbead model is applied.

Plastic strain - Membrane

0.5906
0.5062
0.4218
0.3375
0.2531
0.1687
0.0844
0.0000

With drawbead

without drawbead
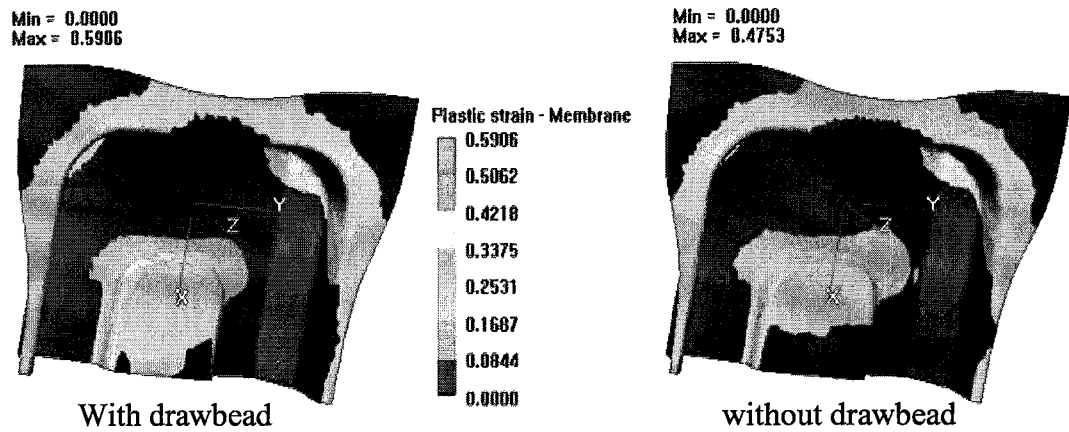
Figure 6.4: Plastic Membrane Strain Distribution in Symmetric Rectangular Product

Springback is one of the key factors to influence on the quality of stamped sheet metal parts. The springback deformation happens on the stamped product after sheet material formed and then punch or blankholder is excluded, so that it occurs a great difference from the desired shape. Therefore, the springback analysis takes charge of an important role in the area of tool design for the sheet metal stamping process as more sophisticated stamped sheet parts are needed nowadays.

The reduction of springback is an effect of increased restraining forces on the blank during drawing. However, changed bending and unbending condition of the sheet during the drawing process induces different tension and compression forces on the upper and lower sheet side [22].

The springback behaviour of the symmetric rectangular product is shown in Figure 6.5 along cross-section A-A' (see Figure 6.2b). In the flange shape of the product, great differences is occured after the springback. When drawbeads are used, the plastic strain distribution in the product is increased (see Figure 6.4), so it is clearly seen from Figure 6.5 that the springback is decreased with using drawbeads. However, increasing restraining forces with using drawbead may also induce cracks.

Die

Blank without drawbeads

Blank with drawbeads
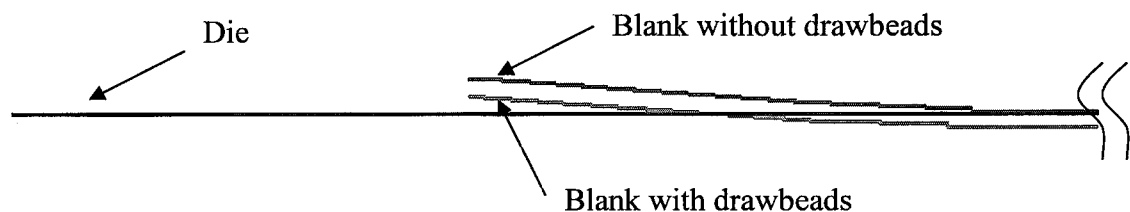
Figure 6.5: Springback Behaviour in the Flange Shape Along the Cross-section A-A'

6.1.1 Evaluation criteria

In this part of this thesis, a criteria namely Forming Limid Diagram (FLD) is introduced in order to evaluate the possibility of wrinkling, cracking etc.,. The Forming Limit Diagram (FLD) represents the formability of the sheet material which is subject to forming deformation. To compare the differences in formability and strength the strain analysis is performed. For strain analysis circle grids are etched on the blank before stamping. After stamping major and minor strains can be measured by determining the shape of the circles (ovals) as in Figure 6.6. The major strain is calculated by the change of the circle diameter in primary deformation direction, minor strain by the change of diameter in secondary deformation direction to determine the deformation capability regarding the distribution, direction and quantity [24].

$$\varepsilon_1 = \ln (l_1/l_0)$$

$$\varepsilon_2 = \ln (l_2/l_0)$$
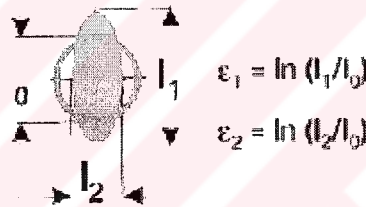
Figure 6.6: Schematic of Circle Grid Deformation

The ellipses that result from the circles during the forming process are measured on major and minor axes. (See Figure 6.7) These measured values which are converted to percentage or logarithmic deformation values related to the diameter of the starting circle are compared against the Forming Limit Curve (FLC), see Figure 6.7. The Forming Limit Curve (FLC) has been used for about twenty years and has yielded numerous successful results. It is traditionally considered as a good indicator for the failure criterion. This curve is extracted from biaxial strain tests, for example via the Erichsen test. The test specimen of the material has been drawn until fracture or diffuse necking.
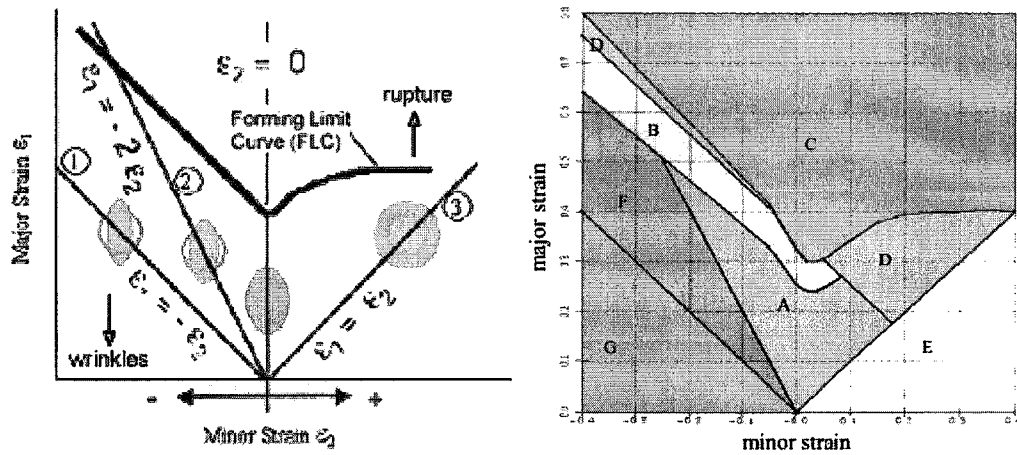
Figure 6.7: FLD Where the Major Strain ϵ_1 is Applied on the Y-Axis and the Minor Strain ϵ_2 is Applied on the X-Axis.

In the (ϵ_2, ϵ_1) space, the forming limit curve (FLC), given by experiments or numerical prediction for each material, limits the safe region. Failure occurs during deep drawing at a material point, if for this point the principal strains (ϵ_2, ϵ_1) are above the FLC.

In the Figure 6.7, the curve that forms the lower boundary of the area C is the forming limit curve. The curve describes the level of strain that the actual material can withstand until failure, cracking or wrinkling occurs. Following a rule of thumb experience to assure that the component not will break the strain level should not exceed 80% of the level of the forming limit curve [25]. The different areas (see Figurre 6.7) in the diagram are:

A. Recommended!. Safe region, appropriate use of the forming abilities of the material

B. Danger of rupture or cracking.

C. The material has cracked.

D. Severe thinning.

E. Insufficient plastic strain, risk of spring back

F. Tendency to wrinkling.

G. Fully developed wrinkles (or thickening).

The results represented in forming limit diagrams (FLDs) as given in Figure 6.8 show the formability characteristics of the rectangular product.

55

FLD (strain) - Zones by quality

- Strong wrinkling trend
- Wrinkling trend
- Insufficient stretching
- Safe
- Excessive thinning
- Cracks

With drawbead   without drawbead
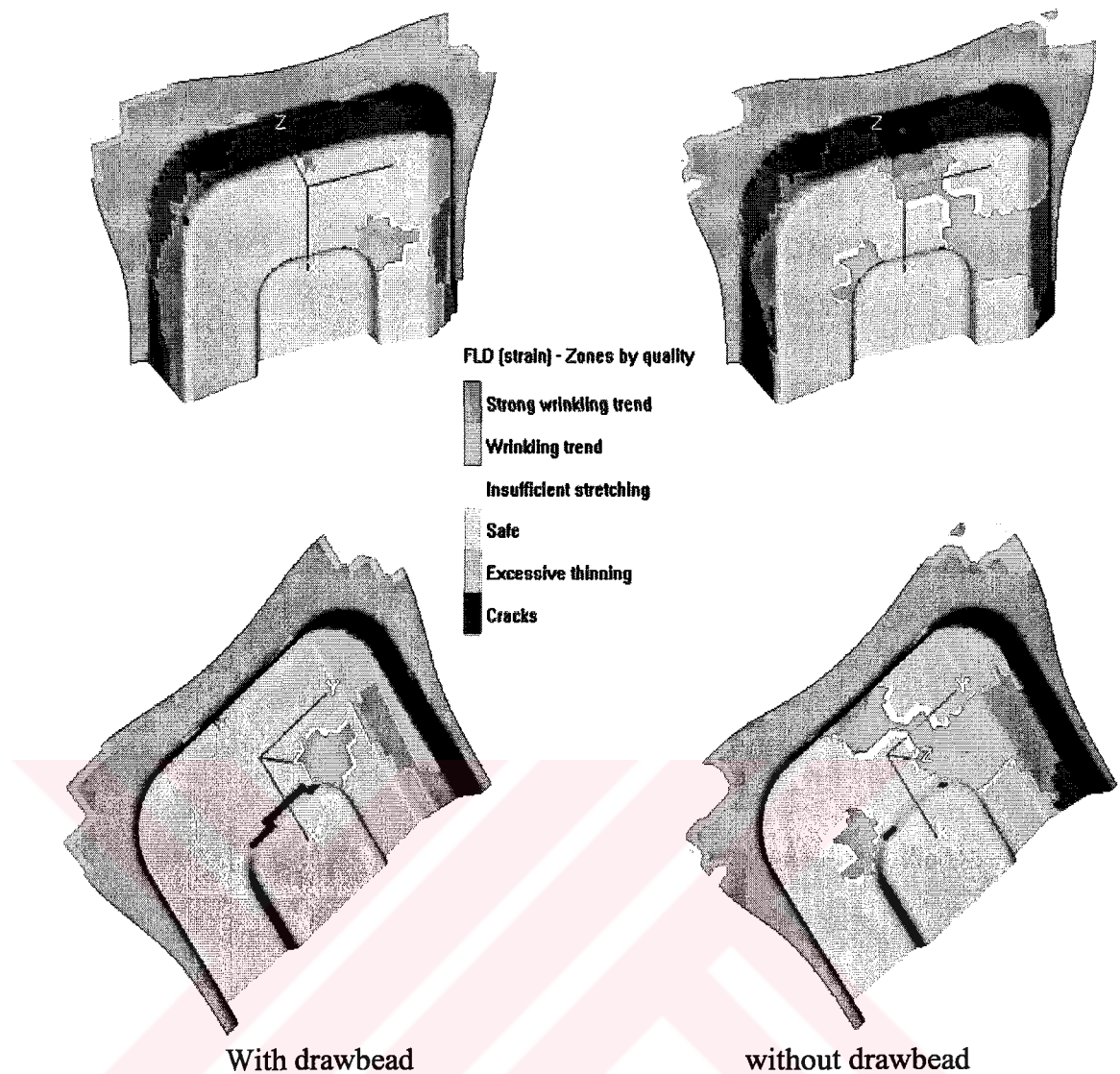
Figure 6.8: FLD Result - Formability of the Symmetric Rectangular Product

Wrinkles are the result of insufficient stretch or uncontrolled compression. It can be concluded from this figure that the wrinkling tendency in the rectangular product is significantly reduced when the equivalent drawbead model is applied. In addition to this, safe region of the product is increased with using drawbeads. In the same way, it can be said that excessive thinning and cracks regions are also increased in the product with drawbeads. These defects may be eliminated with the proper drawbead design and with optimum drawbead forces especially in the regions where the sheet metal cannot easily flow into the die cavity.

The flange shape of the symmetric rectangular product, determined with both simulations, is depicted in Figure 6.9. From this figure, it can be seen that the draw-in at the drawbead position is significantly less when an equivalent drawbead model

is used, which was also expected. In the simulation without drawbead, the material flowed more easily die radius regions into the die cavity since the material flow was only restrained by the blankholder, resulting in a higher draw-in.
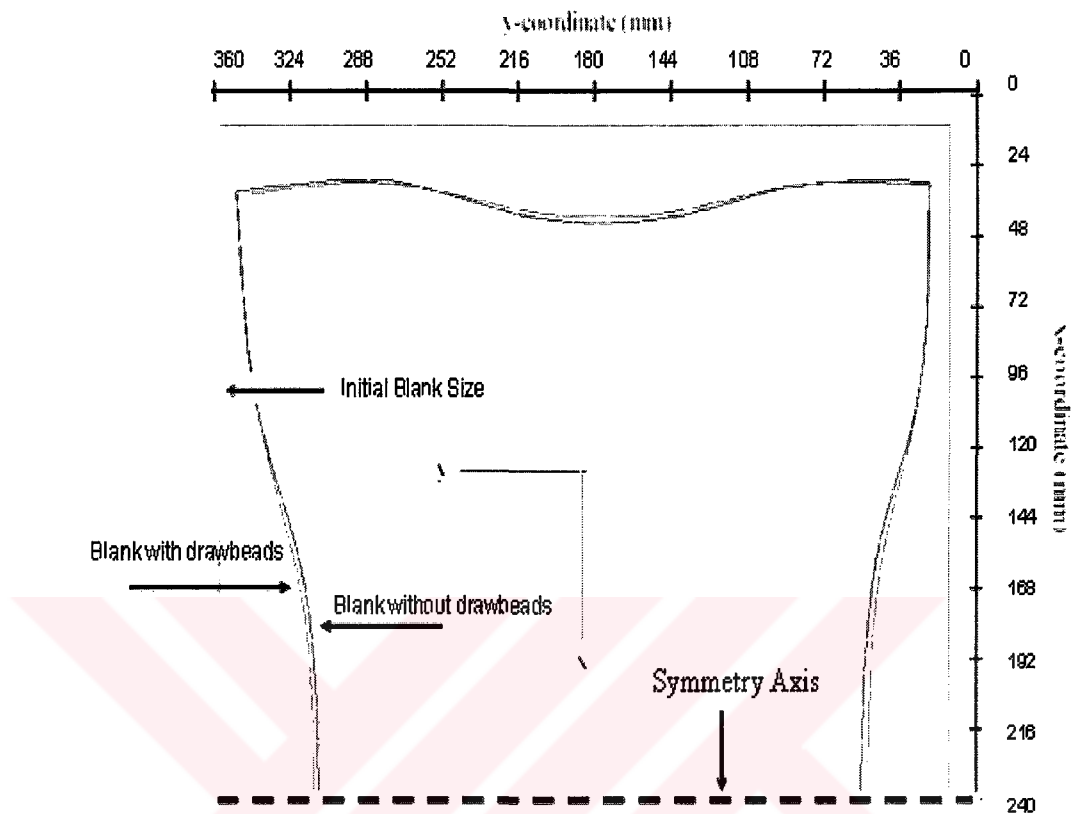
Figure 6.9: Flange Shape of the Rectangular Product After the Forming

The direction of the binder hold down force (BHF), which appears when the material is pulled through the drawbead, is opposite to the blankholder force direction. This BHF causes a rise of the entire blankholder from which it can be concluded that the BHF is not a local phenomenon but will affect the total deep drawing process. The BHF is therefore subtracted from the total blankholder force during the deep drawing simulation.

In the rectangular product case, the total length of the drawbeads was 400 mm and the binder hold down force set as value of 0.05 kN/mm. Therefore the total BHF equals to 400 x 0.05 = 20 kN which tries to lift the blankholder, so this BHF is subtracted from the total blankholder force. The effective blankholder force can be calculated as 50-20 = 30 kN which is agree with the results generated from the simulation in the Figure 6.10.
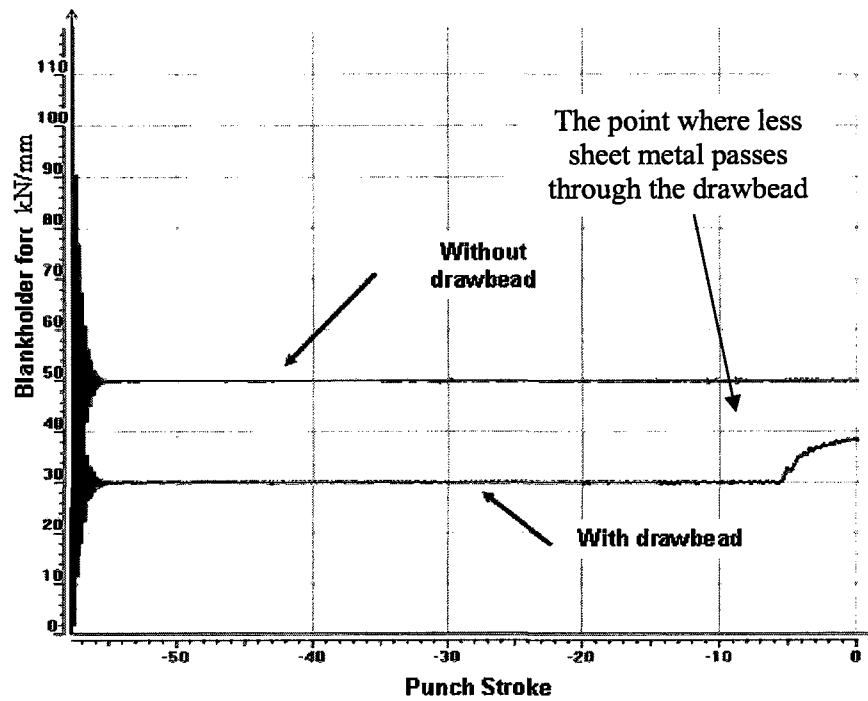
Figure 6.10: Blankholder Force of the Product During the Forming Stage
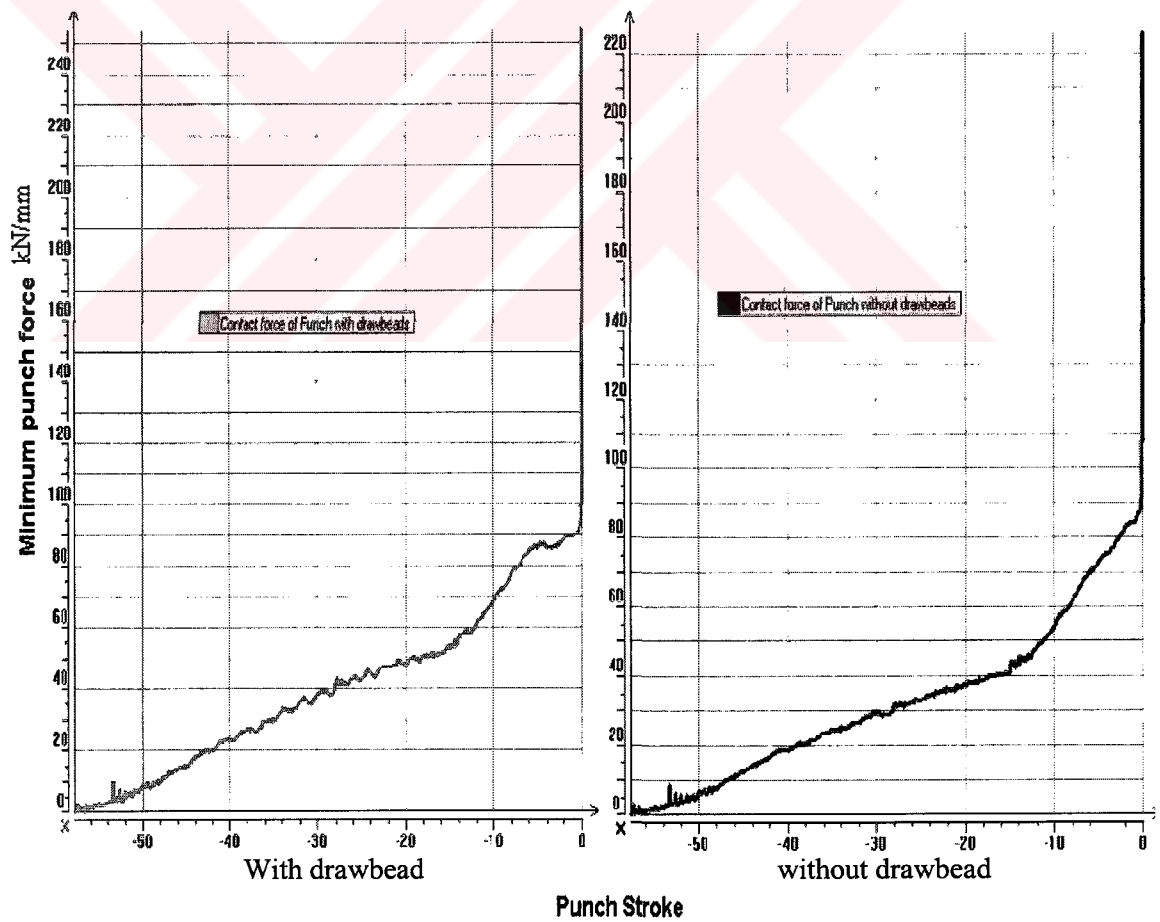
Figure 6.11: Minimum Required Punch Force During the Forming Stage

58

In the same way, minimum required punch force that can complete the simulations will be increased if drawbeads are used. The punch force must overcome the additional binder hold down force. This phenomenon is shown in the Figure 6.11 for the half of the rectangular product. For this reason, if it is required to use drawbead, the tonnage capacity of the press should be recalculated.

6.2 Decklid Inner Panel

In order to evaluate the drawbead behaviour for real automotive parts, the benchmark of Numisheet'2005 is chosen [26]. This benchmark consists of the forming process of the decklid inner panel. The simulations are carried out to demonstrate the performance of the equivalent drawbead modelling technique.

In the decklid inner panel simulation, punch, binder (blankholder) and die are illustrated in Figure 6.12. This tooling geometry has a symmetry plane at x=0. The material used in this simulation is shown in Table 6.2. Total blankholder force is 1334 kN.
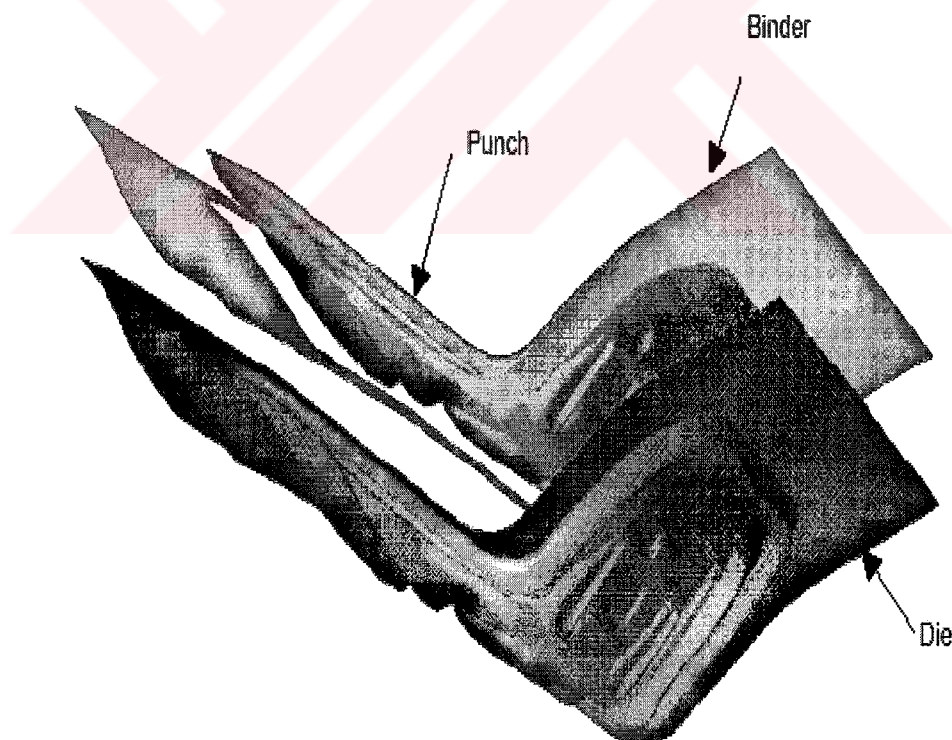
Figure 6.12: Tool Description for the Decklid Inner Panel

Table 6.2: Material Properties for the Decklid Inner Panel

Properties	Value
Yield Stress (MPa)	0.201
Young's Modulus (GPa)	210
Plastic anisotropy parameter, r0	1.604
Plastic anisotropy parameter, r45	1.388
Plastic anisotropy parameter, r90	1.991
Work-hardening exponent	0.195
Coulomb friction coefficient	0.12
Strength coefficient (MPa)	0.554
Poisson's ratio	0.3
Thickness (mm)	0.8

Figure 6.13 shows the drawbead centerlines and the transition points between bead section geometries to be used by equivalent drawbead in the FE simulation. In the Table 6.3, the geometrical parameters are given for these drawbead types as shown in Figure 6.14.
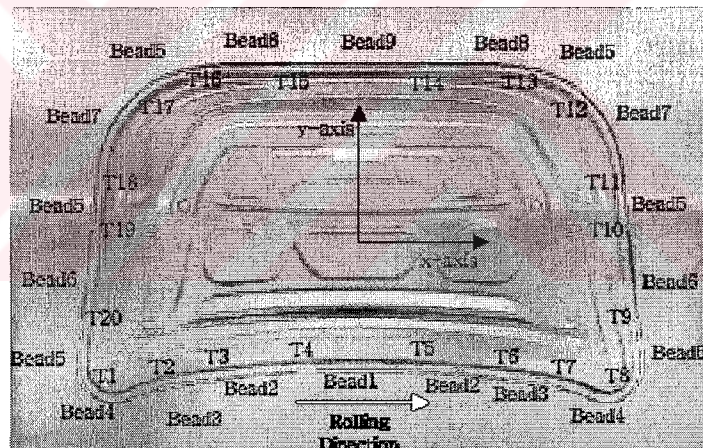
Figure 6.13: Drawbead Centerlines and Transition Points Between Bead Sections
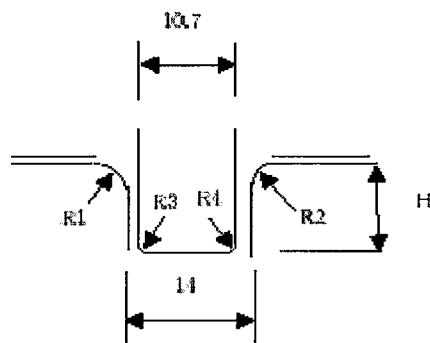
Figure 6.14: Drawbead Section

Table 6.3: Drawbead Section Parameters

Bead #	R1 (mm)	R2 (mm)	R3(=R4) (mm)	H (mm)
Bead1	2.50	2.50	3.0	7.0
Bead2	2.50	2.50	3.0	4.5
Bead3	2.50	2.50	2.5	6.0
Bead4	2.50	2.50	2.5	7.0
Bead5	2.75	2.75	3.0	5.0
Bead6	2.50	2.50	3.0	6.5
Bead7	3.50	3.50	3.5	5.0
Bead8	2.50	2.50	3.0	7.5
Bead9	3.00	3.00	3.5	5.5

In the opposite of Numisheet'2005 benchmark, the double-action simulations are performed which consists of four stages: gravity, holding, forming and trimming as shown in Figure 6.15. The die is stationary.

a- Double action process   b- Gravity stage

c- Holding stage   d- Stamping stage
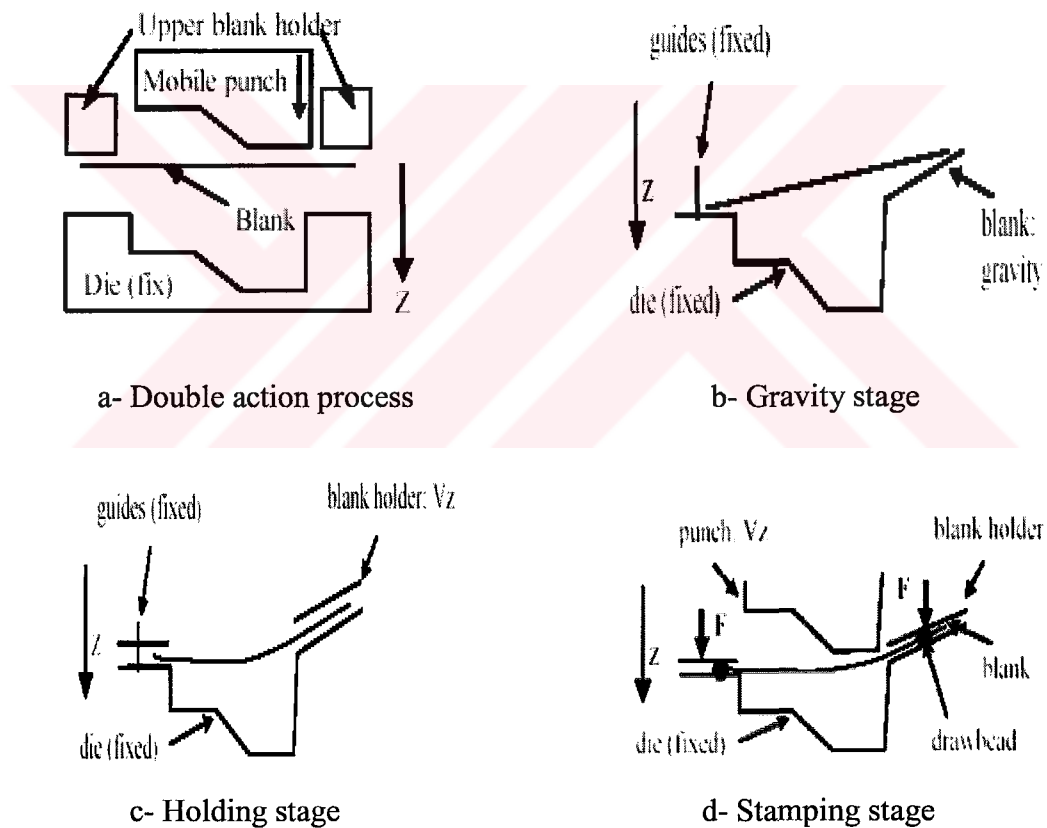
Figure 6.15: Double Action Process Used for the Decklid Inner Panel

After the simulation model is created (including the different tool components, data for the material and process parameters as binder force, punch velocity, etc.) the forming simulation can be conducted according to following steps [23]:

61

- Gravity stage is applied to get the shape or deformation of the metal sheet when it is placed on the binder. It is very important if a thin and large sheet is used.

- Holding stage or closing of the binder is the first step of the forming process. The binder is moved towards the die and forces the sheet against the die.

- Stamping stage, when the punch is moved down in the die and the forming process is simulated.

- Trimming, when scrap is removed from the component.

Three elasto-plastic finite element simulations including the real drawbead geometry and its equivalent representation are performed with the finite element program Pam Stamp 2G v2004 for both the case with real drawbead geometry and its equivalent representation. First simulation is performed in which the real drawbead is modelled and the second simulation is carried out in which the equivalent drawbead is applied and the third one is performed without drawbeads.

The plastic flow under multi-axial stress states is describe by a yield criterion, which is derived directly from data of tests at the key stress-states. In the simulations, Hill-48 which is one of the commonly used yield criteria is used. The discussion of the results obtained will focus on the differences between the results of the simulations.

Figure 6.16 shows the blank deformation during the holding stage for the case with real drawbead and without drawbead. From Figure 6.17, max plastic strain over the thickness for the blank with and without real drawbead is 0.3191 and 0.0459 respectively.
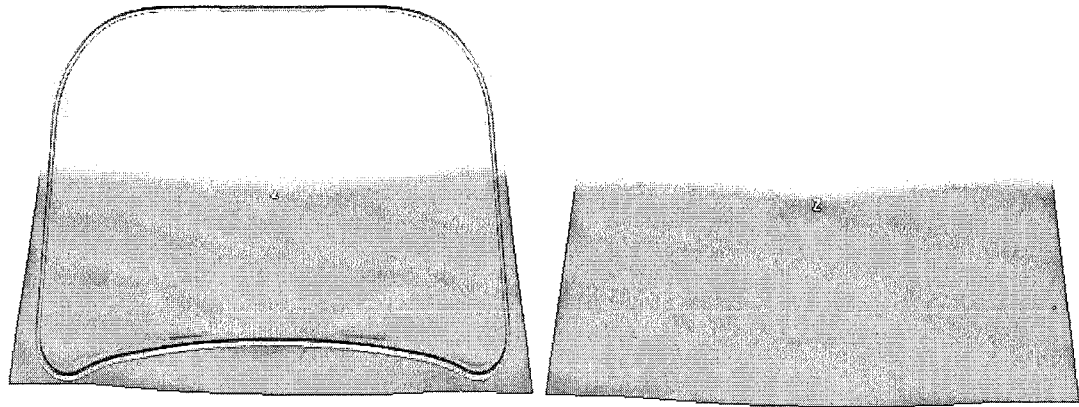
a- With real drawbeads   **b- Without drawbeads**

Figure 6.16: Holding Stage for the Case with
Real Drawbeads and without Drawbeads
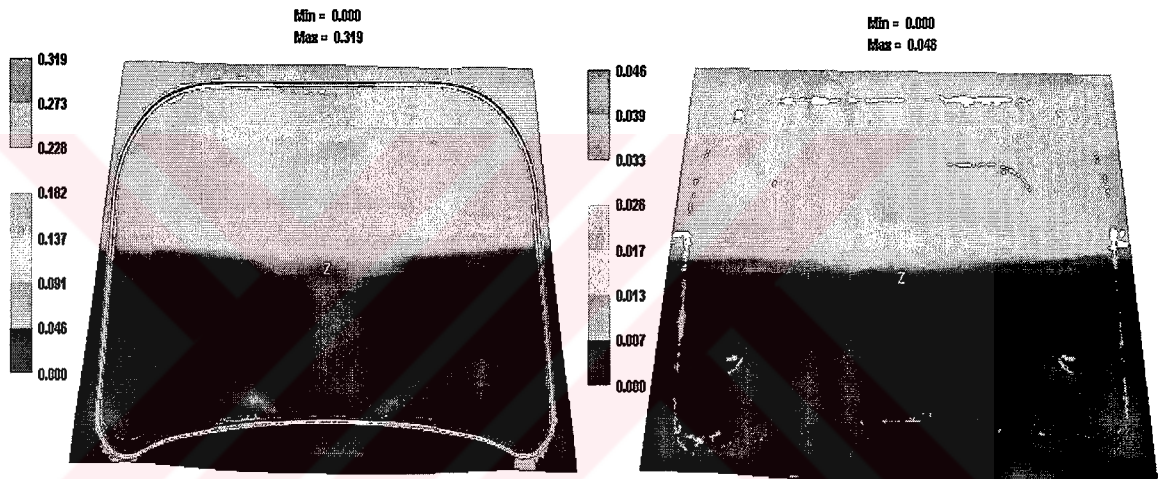
a- With real drawbeads   **b- Without drawbeads**

Figure 6.17: Plastic Strain Distribution Over the Thickness in the Holding Stage for
the Case with Real Drawbeads and Without Drawbeads

Figure 6.18 shows the plastic strain distribution and equivalent stress-state at the end of the stamping stage with trimming operation. The maximum plastic strain for the case with real drawbeads is 1.534 and for the case with equivalent drawbeads and without drawbeads is 1.144 and 0.637 respectively. Maximum equivalent membrane stress for the case with real drawbeads is 0.554 and for the case with equivalent drawbeads and without drawbeads is 0.554 and 0.525 GPa respectively. It is concluded that the strain and stress distribution in the entire product is significantly influenced when the equivalent drawbead model is applied.

Plastic strain - Membrane   **Equivalent stress - Membrane**

The case with real drawbeads

Min = 0.022	Min = 0.206
Max = 1.534	Max = 0.554

The case with equivalent drawbeads

Min = 0.017	Min = 0.188
Max = 1.144	Max = 0.554

The case without drawbeads

Min = 0.000	Min = 0.077
Max = 0.637	Max = 0.525
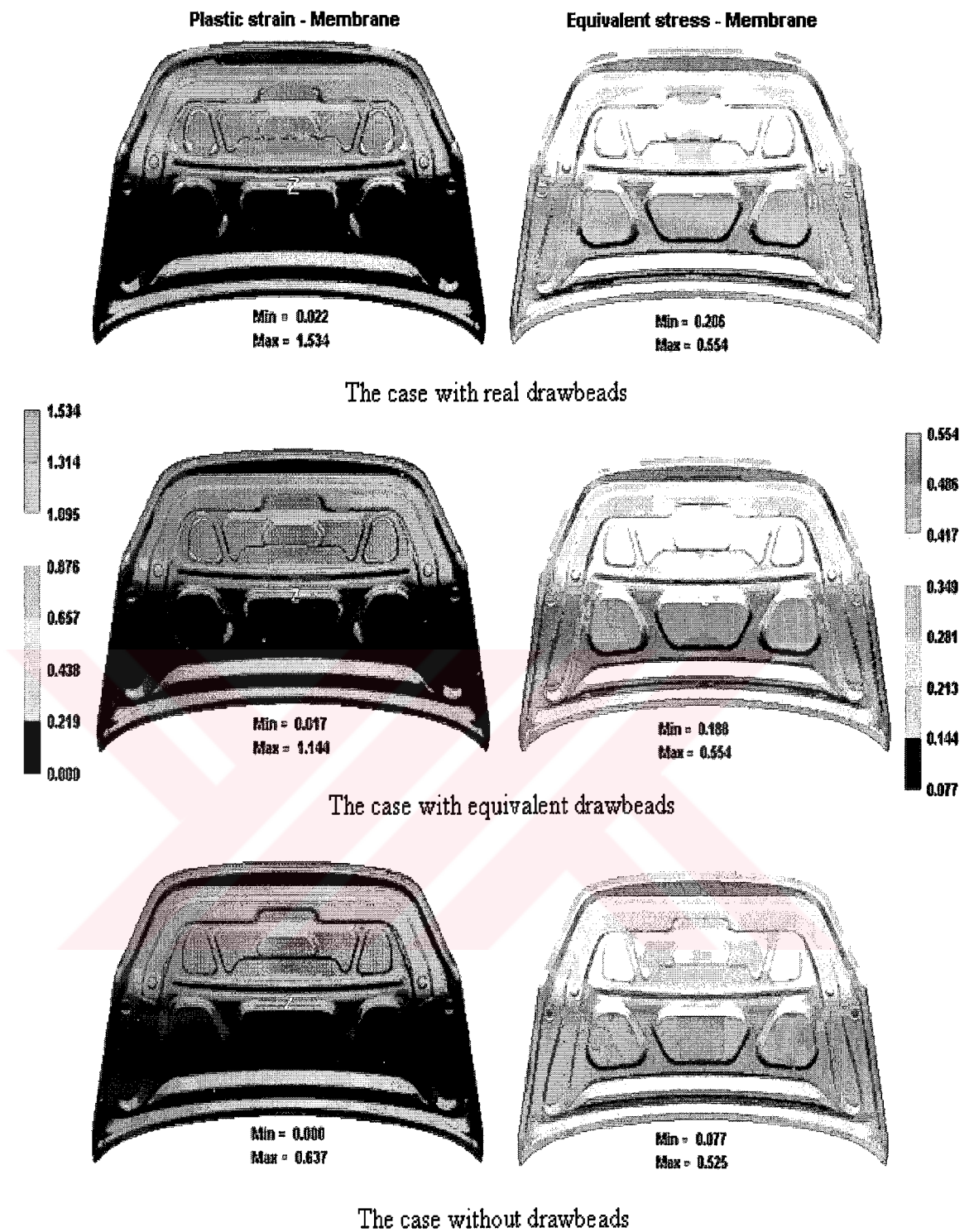
a- Plastic strain-membrane   b- Equivalent stress-membrane

Figure 6.18: a- Plastic Strain- membrane and **b-** Equivalent Stress-membrane Distribution in the Stamping Stage for all Cases

FLD (strain) - Zones by quality

Strong wrinkling trend

Wrinkling trend

Insufficient stretching

Safe

Excessive thinning

Cracks

a-) The case with real drawbeads   b-) The case with equivalent drawbeads   c-) The case without drawbeads
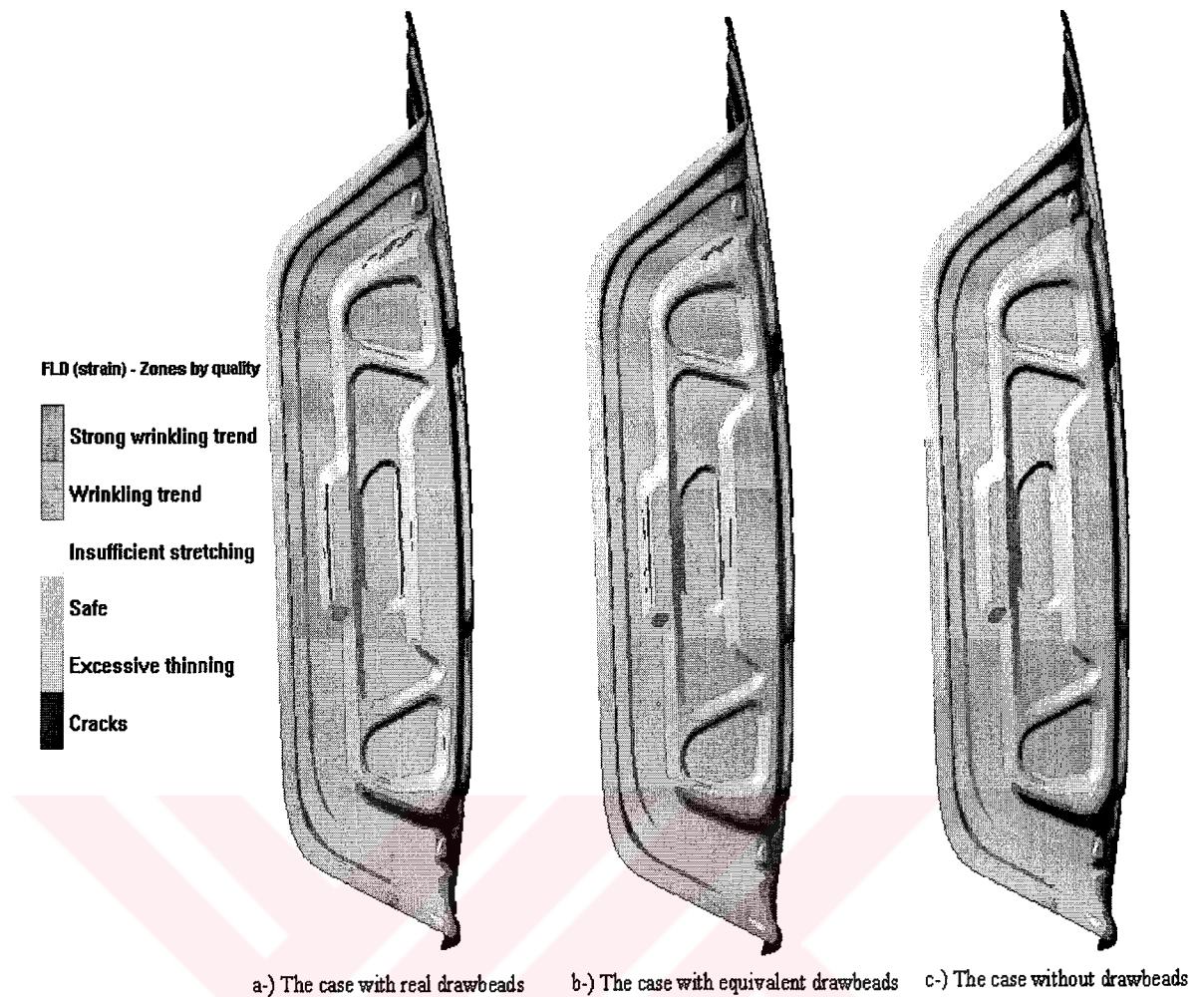
Figure 6.19: Formability of the Decklid Inner Panel

Figure 6.19 and 6.20 show the formability characteristics of the decklid inner panel. It can be concluded from this figure that when the drawbead is taken into account, the wrinkling tendency in the entire product is significantly reduced with respect to the case without drawbead. In addition to this, safe region of the product is increased with using drawbeads. In the same way, it can be said that excessive thinning and cracks regions are also increased in the product with drawbeads.

From Figure 6.18 to 6.120, we observe a good agreement between the two simulations; the case where real drawbead geometries are modelled and the case where equivalent drawbeads are applied. This agreement implies that the equivalent drawbead modelling technique gives similar results with respect to real drawbead.
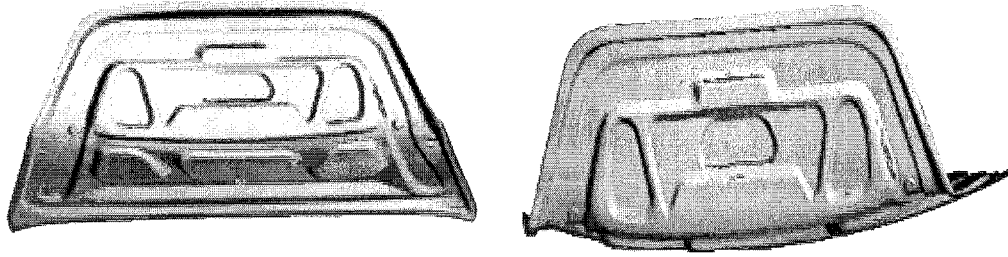
a-) The case with real drawbeads
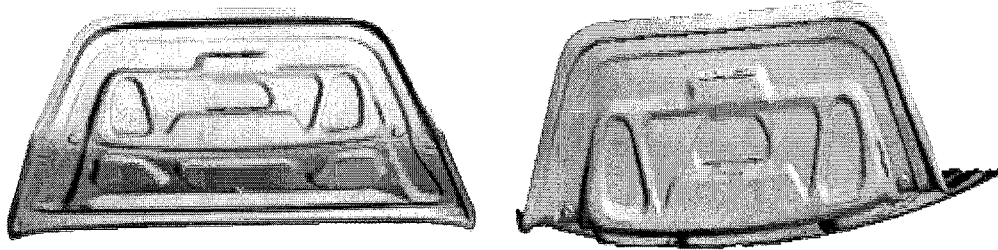
b-) The case with equivalent drawbeads

c-) The case without drawbeads

Figure 6.20: Formability of the Decklid Inner Panel

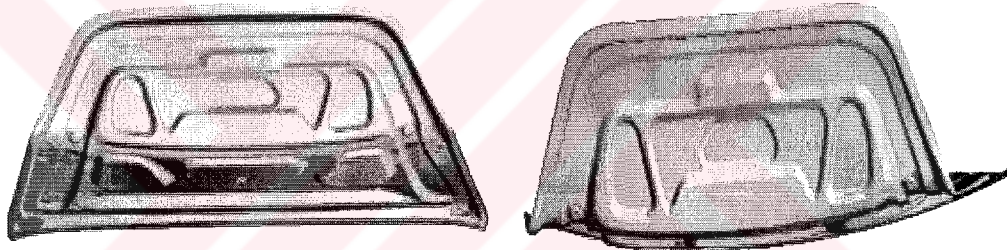It can be concluded that results from the case with real and equivalent drawbead are very similar, thus it can be said that equivalent drawbead method is a reliable predictions tool to estimate the drawbead forces and determination of drawbead behaviour in sheet metal forming simulations.

The border lines of the blank for all simulation cases are depicted in Figure 6.21. From this figure, it can be seen that the draw-in at the drawbead position is very similar and significantly less for the case with real and equivalent drawbead cases which is also expected. In the simulation without drawbead, the material flowed more easily die radius regions into the die cavity since the material flow is only restrained by the blankholder, resulting in a higher draw-in.
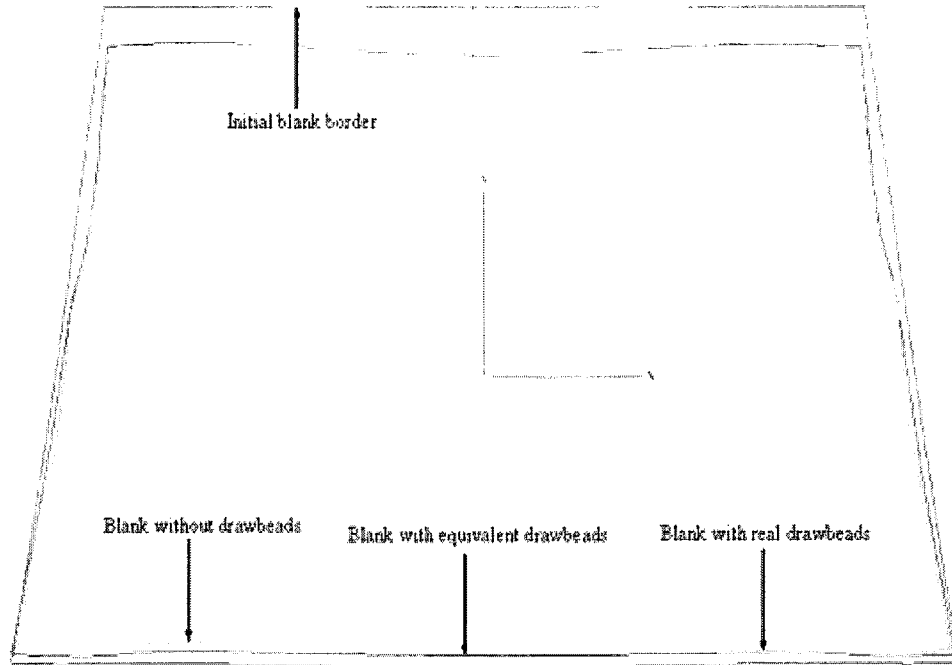
Figure 6.21: Blank Border Lines of the Decklid Inner Panel After the Forming

Table 6.4 shows the computational efforts for all cases which are calculated on Windows-NT computing platform with 3.2 GHz and 2 GB memory. Using equivalent drawbead model avoids the need for using an extremely fine mesh for the sheet metal and, in consequence, a huge saving of computation time can be achieved without significant loss of accuracy. This means that the higher accuracy of the equivalent drawbead modelling does not come at the expense of extra computational time. It is therefore fast enough for complete automotive pressing to be evaluate.

Table 6.4: Summary of the Computational Effort

The case	Number of elements	Number of nodes	CPU time $(10^4 s)$	Total actual memory needed (MB)	Time step (10^3)
with real drawbeads	269,100	267,700	4.69	763	0.554
with equivalent drawbeads	102,200	99,500	2.04	550	0.636
without drawbeads	103,800	101,000	1.96	561	0.647

Furthermore, the equivalent drawbead model has more advantages compared to the use of the real drawbead geometry. The equivalent drawbead is a flexible design tool. The effect of position and geometrical parameters of drawbeads on the material flow can be studied very easily without the necessity to adapt the CAD drawings for a variation in the position or geometry of the real drawbead. Consequently, the equivalent drawbead model is a powerful tool to replace the real drawbead geometry in sheet metal forming simulations without significant loss of accuracy.

7. CONCLUSIONS AND RECOMMENDATIONS

Drawbead design and drawbead force control are one of the most important parameters to control the material flow locally to avoid defects such as wrinkling, tearing, surface distortion and springback and thus the part quality in the sheet metal design and forming process. In this thesis, the guidelines in drawbead design and usage of drawbead are presented and the effects of process variables on drawbead forces are investigated. A number of mathematical models are represented to identify the relationship between the drawbead forces and drawbead geometry. The accuracy and assumptions made in these models are demonstrated. In order to determine the drawbead effects, 3D plane stress and 2D plane strain numerical models are created to be compared with experimental results. A comparison between the experimental and numerical results reveals that the numerical models fit well to the experimental. This proves that the numerical models give reliable predictions of the drawbead forces; drawbead restraining force (DBRF), the binder hold down force (BHF). Therefore, these models can be used to determine the process dependent drawbead forces for all possible drawbead geometries without doing experiment.

In finite element simulations, real drawbead geometries are seldom included because of the small radii. In this thesis, the equivalent drawbead modelling which is used instead of the real drawbead geometries and defined as fixed lines on the tool surface is also presented. A huge saving of computation time and design flexibility can be achieved by using equivalent drawbead in sheet metal forming simulations. In order to put forward the methodologies to obtain the accuracy of equivalent drawbead modelling technique and accurate prediction of drawbead behaviour on stamped part, five numerical models which related to two separate geometries are developed. The results of these models serve as a reference for determination of the equivalent drawbead's performance and the effects of using drawbeads.

69

The results clearly show that using drawbeads reduces wrinkling tendency and increases the strain distribution, this reduces springback and gives sufficient stretching which provide high dent resistance (or flex resistance) especially for large outer panels. It is also seen that simulations with drawbead can be performed under a relatively low blankholder force by changing the restraining force locally. This avoids the problems of exceeding the tonnage capability of the press. Using drawbead gives more uniform deformations, thus fine cutting contour line and high assembly quality can be obtained.

The good agreement between the simulations with real drawbead and with its equivalent drawbead representation shows that the equivalent drawbead model is a powerful tool to replace the real drawbead geometry in sheet metal forming simulations without significant loss of accuracy.

REFERENCES

[1] **Tufekci, S.S, Wang, C.T, Kinzel, G.L, and Taylan, A.,** 1994. Estimation and control of drawbead forces in sheet metal forming, SAE Technical Paper Series-940941, 152-162.

[2] **Meinders T.,** 2000. Developments in numerical simulations of the real life deep drawing process, Ph.D. Thesis, University of Twente, Enschede, Ponsen & Looijen Wageningen (publ.), ISBN 90-36514002.

[3] **Pam Stamp 2G,** Version 2004.1, 2005. PAMSTAMP-2G User's Guide, Parc Club du Golf 13856 Aix en Provence cedex 3 France.

[4] **Keeler S.,** 2000. How we think draw beads work, The Science of Forming, 72-73.

[5] **Kawka, M., Wang, A.,** 1994. Improving drawbeads and friction models simulations of industrial sheet metal forming process, Metal Forming In Industry, conference proceedings, Baden-Baden.

[6] **Cinotti N.,** 2002. Stretch flange formability of aluminum alloy sheet, Ph.D. Thesis, University of Waterloo, Waterloo, Ontario, Canada.

[7] **Keeler S.,** 2000. How draw beads actually work, The Science of Forming, 70-71.

[8] **Yang, Y.Y, Wang, R.F and Wang, Y.Z.,** 2000. 2D elasto-plastic FE simulation of the drawbead drawing process, Journal of Materials Processing Technology, **120,** 17-20.

[9] **Johnson, W and Mellor, P.B.,** 1983. Engineering Plasticity, Ellis Horwood Limited, England.

[10] **Waller, J.A.,** 1978. Drawing and pressing, Pres tools and presswork, Portcullis, Burgess Hill, Great Britain.

[11] **Jung, D.W.,** 2002. Static-explicit finite element method and its application to drawbead process with spring-back, Journal of Materials Processing Technology, **128,** 292-301.

[12] **Wang, N.M, Shah V.C.,** 1991. Drawbead design and performance, J.Materials Shaping Technology, **9,** 21-26.

[13] **Weideman, C.,** 1978. The blankholder action of draw beads, Proc. of 10th Biennial IDDRG Cng, 79-85.

[14] **Eary, DF, Read E.A.,** 1974. Techniques of pressworking sheet metal, Prentice-Hall Inc., Englwood Cliffs, New Jersey.

[15] **Keum, Y.T, Ghoo, B.Y and Kim J.H.,** 2001, Application of an expert drawbead model to the Finite Element Simulation of Sheet forming processes, Journal of Materials Processing Technology, **111**, 155-158.

[16] **Carleer, B.D, Vreede, P.T, Louwes, M.F.M and Huétink, J.,** 1995. Modelling drawbeads in 3D finite element simulations of the deep drawing process, Numiform conference proceedings, 681-685.

[17] **Courvoisier, L, Martiny, M, Ferron, G.,** 2002. Analytical modelling of drawbead in sheet metal forming, Journal of Materials Processing Technology, **133**, 359-370.

[18] **Naceur, H, Guo, Y.Q, Batoz, J.L and Knopf-Lenoir, C.,** 2001. Optimization of drawbead restraining forces and drawbead design in sheet metal process, Journal of Materials Processing Technology, **43**, 2407-2434.

[19] **Painter, M.J, Pearc, R.,** 1976. Metal flow through a drawbead, Sheet Metal Industries, July, 1976, 12-19.

[20] **Samuel, M.,** 2001. Influence of drawbead deometry on sheet metal forming, Journal of Materials Processing Technology, **122 (2002)**, 94-103.

[21] **Abaqus/Standard.,** Version 6.5.4 Manuals, 2005. Abaqus Inc., Pawtucket, RI.

[22] **ESI Group.,** 1999. PAMSTAMP Technical Papers, Parc Club du Golf 13856 Aix en Provence cedex 3 France.

[23] **Pam Stamp 2G**, Version 2004.1, 2005. PAMSTAMP-2G Reference Manual, Parc Club du Golf 13856 Aix en Provence cedex 3 France.

[24] **Levy, B.S.,** 2002. Enhanced forming limit diagram project team research report, D.E. Green of Industrial Research and Development Institute, Southfield, MI 48075-1123.

[25] **Keeler, S.,** 2003. Enhanced forming limit diagram project team research report, Keeler Technologies LLC, Southfield, MI 48075-1123.

BIBLIOGRAPHY

Orhan ÇİÇEK was born in Istanbul at 1978. He enrolled Aerounautical and Aerospace Department of Istanbul Technical University in 1996. He was graduated from this department in 2001. His master education at Solid Mechanics Program of the Mechanical Engineering Department in ITU is going on and he also works as process engineer at the Tool & Die and Prototype Manufacturing Department in Ford-Otosan.